

# **Development of Layered Double Hydroxide and PDMS-Based Triboelectric Nanogenerator for Efficient Nano Energy Harvesting**



By

Fatima Rehan

(Registration No: 00000401196)

Department of Materials Engineering

School of Chemical and Materials Engineering

National University of Sciences & Technology (NUST)

Islamabad, Pakistan

(2024)

# **Development of Layered Double Hydroxide and PDMS-Based Triboelectric Nanogenerator for Efficient Nano Energy Harvesting**



By

Fatima Rehan

(Registration No: 00000401196)

A thesis submitted to the National University of Sciences and Technology, Islamabad,

in partial fulfillment of the requirements for the degree of

Master of Science in

Nanoscience and Engineering

Supervisor: Dr. Muhammad Irfan

School of Chemical and Materials Engineering

National University of Sciences & Technology (NUST)

Islamabad, Pakistan


(2024)

# THESIS ACCEPTANCE CERTIFICATE



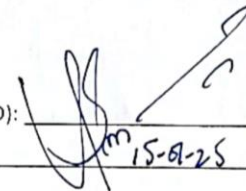
## THESIS ACCEPTANCE CERTIFICATE


Certified that final copy of MS Thesis entitled "Development of Layered Double Hydroxide and PDMS-Based Triboelectric Nanogenerator for Efficient Nano Energy Harvesting" written by Ms Fatima Rehan (Registration No 00000401196), of School of Chemical & Materials Engineering (SCME) has been vetted by undersigned, found complete in all respects as per NUST Statues/Regulations, is free of plagiarism, errors, and mistakes and is accepted as partial fulfillment for award of MS degree. It is further certified that necessary amendments as pointed out by GEC members of the scholar have also been incorporated in the said thesis.

Signature:   
15/1/25

Name of Supervisor: Dr Muhammad Irfan

Date: \_\_\_\_\_

Signature (HOD):   
Date: 15-8-25

Signature (Dean/Principal):   
Date: 15/1/25

# TH-1

NSE-10-2022

Form TH-1

## National University of Sciences & Technology (NUST) MASTER'S THESIS WORK

Name: Fatima Rehan  
Department: Department of Materials Engineering  
Credit Hour Completed: 24.0  
Course Work Completed

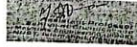


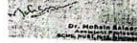
Formulation of Guidance and Examination Committee (GEC)  
NUST Reg No: 00000401196  
Specialization: Master of Science in Nanoscience and Engineering  
CGPA: 3.06

S/No:	Code:	Title:	Core/Elective:	CH:	Grade:
1.	NSE-813	Essentials of Nanoscience and Engineering	Compulsory	3.0	B
2.	MSE-854	Characterization Of Materials	Compulsory	3.0	B
3.	NSE-843	Nano Technology And Photovoltaics	Elective	3.0	C+
4.	MSE-856	Nano Material and Processing	Compulsory	3.0	B
5.	ESE-836	Li-ion and Next Generation Batteries	Elective	3.0	B
6.	RM-898	Research Methodology	Additional	2.0	Q
7.	NSE-941	Nano Composite Materials	Elective	3.0	B
8.	NSE-842	Nano Materials For Energy Applications	Elective	3.0	B+
9.	NSE-845	Nanolithography And Device Fabrication	Elective	3.0	B+


Date 18-Apr-2024

Student's Signature Fatima Rehan

### Thesis Committee

- Name: Muhammad Irfan (Supervisor)  
Department: Department of Materials Engineering  
Signature 
- Name: Usman Khan (Cosupervisor)  
Department: Department of Integrated Circuit & System (ICS-EE)  
Signature U. Khan
- Name: Nabeel Ahmad (Internal)  
Department: Department of Materials Engineering  
Signature 
- Name: Malik Adeel Umer (Internal)  
Department: Department of Materials Engineering  
Signature 
- Name: Mohsin Saleem (Internal)  
Department: Department of Materials Engineering  
Signature 

Date: 18-Apr-2024

Signature of Head of Department: 

### APPROVAL

Date: 18-Apr-2024

Signature of Dean/Principal: 

TH-4



National University of Sciences & Technology (NUST)

FORM TH-4

MASTER'S THESIS WORK

We hereby recommend that the dissertation prepared under our supervision by

Regn No & Name: 00000401196 Fatima Rehan

Title: Development of Layered Double Hydroxide and PDMS-Based Triboelectric Nanogenerator for Efficient Nano Energy Harvesting.

Presented on: 19 Dec 2024 at: 1130 hrs in SCME

Be accepted in partial fulfillment of the requirements for the award of Masters of Science degree in Nanoscience & Engineering.

Guidance & Examination Committee Members

Name: Dr Mohsin Saleem

Signature: Mohsin

Name: Dr Malik Adeel Umer

Signature: Adel

Name: Dr Nabeel Ahmad

Signature: Nabeel

Name: Dr Usman Khan (Co-Supervisor)

Signature: Usman

Supervisor's Name: Dr Muhammad Irfan

Signature: M. Irfan

Dated: 10/01/2025

[Signature]  
Head of Department

Date \_\_\_\_\_

14-01-25

Date

COUNTERSIGNED

[Signature]  
15/1/25

Dean/Principal

School of Chemical & Materials Engineering (SCME)

## **AUTHOR'S DECLARATION**

I Fatima Rehan\_ hereby state that my MS thesis titled “Development of Layered Double Hydroxide and PDMS-Based Triboelectric Nanogenerator for Efficient Nano energy Harvesting ” is my own work and has not been submitted previously by me for taking any degree from National University of Sciences and Technology, Islamabad or anywhere else in the country/ world.

At any time if my statement is found to be incorrect even after I graduate, the university has the right to withdraw my MS degree.

Name of Student: Fatima Rehan

Date: January 9<sup>th</sup>, 2025.

## PLAGIARISM UNDERTAKING

I solemnly declare that research work presented in the thesis titled “**Development of Layered Double Hydroxide and PDMS-Based Triboelectric Nanogenerator for Efficient Nano energy Harvesting**” is solely my research work with no significant contribution from any other person. Small contribution/ help wherever taken has been duly acknowledged and that complete thesis has been written by me.

I understand the zero-tolerance policy of the HEC and National University of Sciences and Technology (NUST), Islamabad towards plagiarism. Therefore, I as an author of the above titled thesis declare that no portion of my thesis has been plagiarized and any material used as reference is properly referred/cited.

I undertake that if I am found guilty of any formal plagiarism in the above titled thesis even after award of MS degree, the University reserves the rights to withdraw/revoke my MS degree and that HEC and NUST, Islamabad has the right to publish my name on the HEC/University website on which names of students are placed who submitted plagiarized thesis.

Student Signature:

A handwritten signature in black ink, appearing to read 'Fatima Rehan', with a horizontal line underneath.

Name: Fatima Rehan.

## **DEDICATION**

*"I dedicated this thesis work to Allah **"The Creator"** (SubhanahuWaTa'ala) almighty, my beloved father and mother, my soulmate, siblings whose love, presence and unwavering support have been the cornerstones of my life. I am certain they would be filled with immense joy to witness my achievement of completing a Master in Nanoscience Engineering from SCME (NUST). I cherish every memory and lesson they bestowed upon me, and I carry their spirit in every challenge I overcome."*



## ACKNOWLEDGEMENT

Humbled and honored thanks to the greatest: **ALLAH** for giving us the strength, knowledge of creation and persistence with grand designs that serve humanity. I offer my sincerest thanks to Almighty Allah, the Lord of all worlds; Whose guidance has always been a source of motivation for me.

I am truly grateful to my advisor **Dr. Muhammad Irfan** who has guided me so clearly and patiently, I am also very thankful to my GEC members **Dr. Usman Khan, Dr. Mohsin Saleem, Dr Nabeel Ahmed** and **Dr. Malik Adeel Umer**, for their kind encouragement and appreciative comments during the whole research work of my journey. I would also like to thank Dr. Usman Khan for co-supervising my project. I also thank Dr. Mohsin Saleem for his immense support and sincere guidance from the start of my thesis to the end, by heart and soul.

I would also like to thank the Materials Engineering Department, Research Hub of SCME for providing all accessible resources and platform at a certain level as conducted my experimentations which contributed to gaining more intellectual research capabilities. Grateful acknowledgement for this technical support goes to the Higher Education Commission (HEC) of Pakistan, which funded through National Research Program for Universities NRPU under Project. No. 20-14492/NRPU/R&D/HEC/2021 entitled "Nanogenerators for self-powered IoT".

I would like to express my deepest gratitude to my beloved soulmate, **Muhammad Saad Ur Rahman**, whose unwavering support, patience, and encouragement have been invaluable throughout this journey. Her assistance in both lab work and paperwork has been instrumental in the completion of this dissertation. And finally, I would like to thank my parents, family, and friends. The support, prayers and beautiful well wishes have truly been our strength.

**Fatima Rehan**

# CONTENTS

<b>ACKNOWLEDGEMENT</b> .....	ix
<b>LIST OF TABLES</b> .....	xii
<b>LIST OF FIGURES</b> .....	xiii
<b>LIST OF ABBREVIATIONS</b> .....	xiv
<b>ABSTRACT</b> .....	xv
<b>CHAPTER 1: INTRODUCTION</b> .....	1
<b>1.1 Motivation</b> .....	1
<b>1.2 Mechanical Energy Harvesting</b> .....	1
<b>1.2.1 Piezoelectric Harvesting</b> .....	1
<b>1.2.2 Electromagnetic Energy Harvesting</b> .....	3
<b>1.2.3 Triboelectric Nanogenerators (TENGs)</b> .....	4
<b>1.3 Triboelectricity</b> .....	5
<b>1.3.1 Triboelectric Series</b> .....	6
<b>1.3.2 Theory of Triboelectricity</b> .....	7
<b>1.3.2.1 Electron Transfer</b> .....	7
<b>1.3.2.2 Ion Transfer</b> .....	9
<b>1.3.2.3 Material Transfer</b> .....	10
<b>1.4 Operational Modes of TENG</b> .....	11
<b>1.4.1 Contact Separation Mode</b> .....	11
<b>1.4.2 Lateral Sliding Mode</b> .....	12
<b>1.4.3 Single Electrode Mode</b> .....	13
<b>1.4.4 Free-Standing Electrode Mode</b> .....	13
<b>1.5 Problem Statement</b> .....	13
<b>1.5 Choice of Materials</b> .....	15
<b>1.6.1 ZnAl-LDH</b> .....	15
<b>1.6.2 MgAl-LDH</b> .....	16
<b>1.6.3 PDMS Stacking on LDH</b> .....	16
<b>1.7 AIMS AND OBJECTIVES</b> .....	18
<b>CHAPTER 2: LITERATURE REVIEW</b> .....	19

<b>2.1</b>	<b>History</b> .....	19
2.1.1	Patterning PDMS by Lithography .....	20
<b>2.1.2</b>	<b>Patterning PDMS by Micro needling</b> .....	21
<b>2.1.3</b>	<b>Patterning PDMS by Sputtering</b> .....	22
<b>2.1.4</b>	<b>Patterning PDMS by Direct Laser</b> .....	23
<b>2.2</b>	<b>State of Art</b> .....	25
<b>CHAPTER 3: MATERIAL AND METHODS</b> .....		26
<b>3.1</b>	<b>Synthesis Route</b> .....	26
<b>3.2</b>	<b>Materials and Apparatus Required</b> .....	26
<b>3.3</b>	<b>Synthesis of ZnAl-LDH and MgAl-LDH</b> .....	27
<b>3.4</b>	<b>Fabrication of TENG</b> .....	30
<b>3.4</b>	<b>Characterization Techniques</b> .....	31
3.4.1	Scanning Electron Microscopy (SEM) .....	31
3.4.2	X-Ray Diffraction (XRD).....	31
3.4.3	Fourier Transform Infrared (FTIR).....	31
3.4.5	Digital Oscilloscope .....	32
<b>CHAPTER 4: RESULTS AND DISCUSSION</b> .....		34
<b>4.1</b>	<b>Materials Characterizations</b> .....	34
4.2.1	Fabrication of Triboelectric Nanogenerators .....	43
<b>4.3</b>	<b>Electrical Characterization and Electronic Interface Circuit of the Triboelectric Nanogenerator</b> .....	44
4.3.1	Electrical Characterization of Triboelectric Nanogenerator .....	44
4.3.2	Electronic Interface Circuit for Triboelectric Sensing of Biomechanical Motions	49
4.3.2.1	A. Electrical Equivalent of Triboelectric Nanogenerator .....	50
4.3.2.2	B. Two-Stage-Amplifier Based Electronic Interface Circuit .....	50
<b>4.4</b>	<b>Step Sensing Application</b> .....	51
<b>Chapter 5: Conclusion and Future Recommendations</b> .....		53
<b>5.1</b>	<b>Conclusion</b> .....	53
<b>5.2</b>	<b>Future Recommendations</b> .....	54
<b>REFERENCES</b> .....		55

## LIST OF TABLES

Table 1: Literature Comparison.....	24
-------------------------------------	----

## LIST OF FIGURES

<b>Figure 1.1:</b> Schematic of Piezoelectric energy harvesting system [1].	2
<b>Figure 1.2:</b> Schematic of Electromagnetic energy harvesting system[2].	3
<b>Figure 1.3:</b> a) Dielectric energy harvesting schematic with charge separation between electrode layers. (b) Mold assembly setup with lock-plate, bolt, and mold-attached plate. (c) Stepwise mold fabrication process for the dielectric layer [3].	5
<b>Figure 1.4:</b> Schematic of Triboelectric series[4].	7
<b>Figure 1.5:</b> Schematic of Electron Transfer in TENG	8
<b>Figure 1.6:</b> Schematic of ion Transfer in TENG	9
<b>Figure 1.7:</b> Schematic of Material Transfer in TENG	10
<b>Figure 1.8:</b> Schematic of Contact Separation Mode	12
<b>Figure 3.1:</b> Schematic of LDH film preparation.	28
<b>Figure 3.2:</b> Digital image of LDH Film	29
<b>Figure 3.3:</b> Schematic of PDMS stacking and curing on LDH film.	29
<b>Figure 3.4:</b> Prototyping and working mechanism of TENG device.	30
<b>Figure 4.1:</b> XRD diffractogram of ZnAl-LDH.	34
<b>Figure 4.2:</b> SEM images of ZnAl-LDH.	35
<b>Figure 4.3:</b> EDS of ZnAl-LDH.	36
<b>Figure 4.4:</b> SEM images of MgAl-LDH.	37
<b>Figure 4.5:</b> EDS of MgAl-LDH.	37
<b>Figure 4.6:</b> SEM images of PDMS stack on LDH surface.	38
<b>Figure 4.7:</b> EDS of PDMS/ZnAl-LDH sample.	39
<b>Figure 4.8:</b> FTIR graph of ZnAl-LDH.	40
<b>Figure 4.9:</b> TGA Graph of pristine ZnAl-LDH.	42
<b>Figure 4.10:</b> TGA graph of PDMS/ZnAl-LDH Composite sample.	42
<b>Figure 4.11:</b> Graph of Output Voltage $V_O$ and Short circuit current $I_{SC}$ of PDMS-AL TENG	45
<b>Figure 4.12:</b> Short Circuit current $I_{SC}$ of PDMS/ZnAl-LDH to Al TENG	46
<b>Figure 4.13:</b> Output Voltage $V_O$ at different load resistance for PDMS/ZnAl-LDH to Al TENG	47
<b>Figure 4.14:</b> $V_O$ and $I_O$ at different Load of ZnAl-LDH/PDMS-Al TENG	48
<b>Figure 4.15:</b> Charge Discharge graph for ZnAl-LDH/PDMS-Al TENG	48
<b>Figure 4.16:</b> Schematic of Triboelectric equivalent circuit	50
<b>Figure 4.17:</b> Digital camera image of integrated TENG in Shoe and tests for step sensing application	52

## LIST OF ABBREVIATIONS

TENG	Triboelectric Nanogenerator
LDH	Layered Double Hydroxide
PDMS	Polydimethylsiloxane
SEM	Scanning Electron Microscopy
FTIR	Fourier transform infrared spectroscopy
TGA	Thermal Gravimetric Analysis
DI	Deionized Water
°C	Degree Centigrade
Nm	Nanometer
NUST	National University of Science and Technology

## ABSTRACT

The energy harvesting of the triboelectric nanogenerators (TENGs) stands as a pragmatic energy harvesting system capable of powering itself without external power sources but progress towards commercialization has been limited due to challenges like low energy conversion efficiency and material dependency. In this work, the challenges stated are tackled in the development of a composite TENG made of Layered double hydroxide (LDH) and polydimethylsiloxane (PDMS) material. The LDH was synthesized using hydrothermal method that resulted to nanostructure porous material with high surface area. Synthesis of ZnAl-LDH was done through X-ray Diffraction (XRD) and was able to show crystalline structure and Scanning Electron Microscopy (SEM) was used to provide insight on the morphology enhancement of the material. There was significant increase on the electrical performance of the composite ZnAl-LDH/PDMS TENG when compared to pristine PDMS with output voltages increasing from 25 V to 30 V and short-circuit current from 20  $\mu$ A to 40  $\mu$ A. Surface roughness and charge storage capacity contributed to the improvement in triboelectric performance which was modulated by the ZnAl-LDH template and hence improved the charge generation and throughput during the contact-separation mechanism. It was further demonstrated that the ZnAl-LDH/PDMS TENG, when paired with a 4.7 $\mu$ F capacitor, successfully charged it to 100V within one hundred seconds, highlighting its potential as an energy storage device. The ability to combine PDMS and ZnAl-LDH resulted in a synergistic effect that enhanced energy conversion as well as the durability of the devices. The aim of this study has been to create a low-cost and efficient energy harvester device which could help in addressing increasing energy needs. A triboelectric nanogenerator (TENG) was fabricated for energy harvesting and demonstrated as a step-sensing device. The polymers and templates employed can be customized to meet emerging demands, such as powering small-scale electronics or scaling up for industrial energy harvesting applications. Further research may focus on optimizing LDH compositions and advancing the scalability of this technology to enhance the versatility and efficiency of TENGs in energy harvesting systems.

**Keywords:** Triboelectric nanogenerators, Triboelectric sensor, Layered Double Hydroxide, Biomechanical motion.



# CHAPTER 1: INTRODUCTION

## 1.1 Motivation

Need for Energy is continuously increasing worldwide, and conventional approaches to supplying it are not sustainable from an environmental standpoint, The movement toward renewable energy sources has accelerated as a result. This is due to dwindling fossil fuel resources and increased campaigns, globally, for cleaner environments through reduced emission of greenhouse gases. In the last few years, Triboelectric nanogenerators (TENGs) are accepted as the novel technique to scavenge mechanical energy from our daily movements and operations, oscillations, and wind and water currents [1].

Nonetheless, there are several issues which need to be addressed to make optimal use of TENGs for efficient, durable, and large-scale energy harvesting applications. The efficiency of TENGs highly depends on the choice of material used as the triboelectric layers. This work shows that high charge density, long-lasting and mechanical flexibility can be attained by using appropriate materials that can effectively generate charges and store them to support the triboelectric effect.

## 1.2 Mechanical Energy Harvesting

Mechanical energy harvesting involves converting mechanical energy from various sources, such as vibrations, motion, and environmental forces into electrical energy. This process is getting a proportional value in modern technology in cases of low power electronics like nanogenerators, wearable technologies, and IoT. This also forms part of the quest to minimize reliance on conventional power sources to derive energy which in turn leads to a sustainable energy future [2].

### *1.2.1 Piezoelectric Harvesting*

The conversion of mechanical energy to electrical is another important mechanism of energy harvesting where the piezoelectric effect is both explored and implemented. It

occurs in specialized materials like quartz, lead zirconate titanate or PZT, and other piezoelectric ceramics, which produce electrical charges from mechanical stress or strain. This effect has been used broadly in conditions where stochastic vibrations or mechanical movements are experienced, for instance in industrial machines, transportation means, and in biomedical applications [3].

In **Figure 1.1** Lead zirconate titanate (PZT) is one of the most widely used piezo materials in piezoelectric energy harvesters due to the large values of its piezoelectric coefficients. When coupled with mechanical vibrations, the PZT-based harvesters generate an electric charge that can either be capacitively stored or directly utilized in supplying energy to small loads. For instance, piezoelectric harvesters are capable to producing power densities of up to  $15 \mu\text{W}$  when mounted in low-frequency vibrations ( $\sim 50 \text{ Hz}$ ). This makes them suitable for use in low power density nanogenerator systems, even in the field of wearable technology [4].

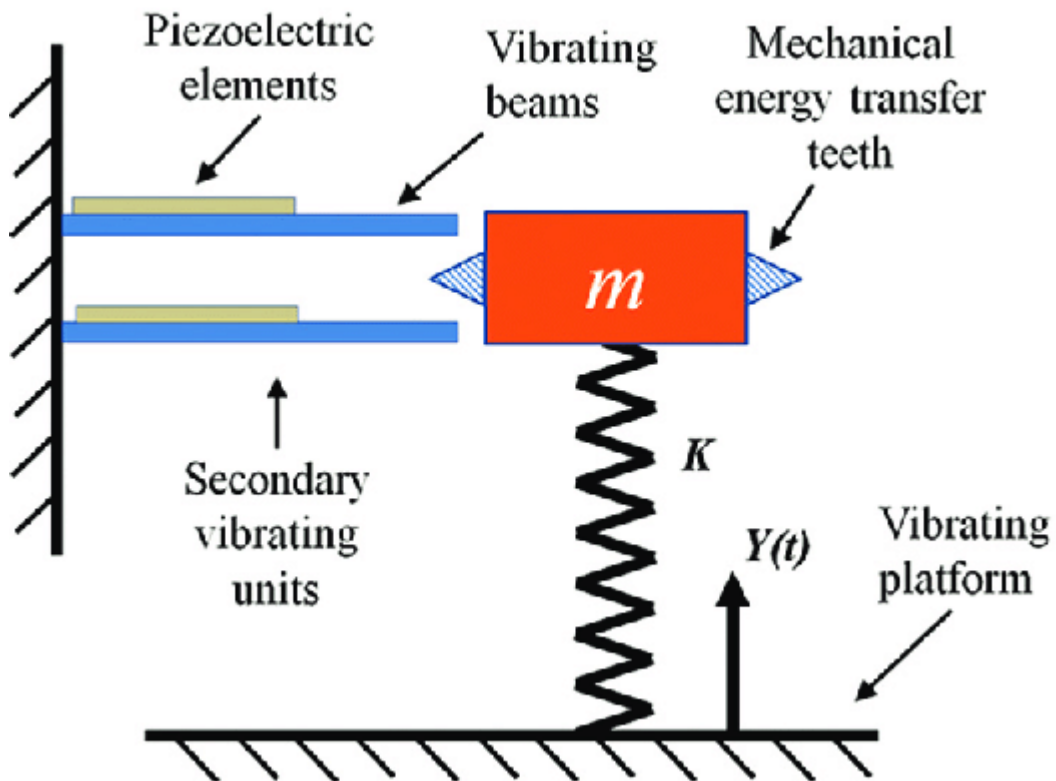


**Figure 1.1:** Schematic of Piezoelectric energy harvesting system [1].

### 1.2.2 Electromagnetic Energy Harvesting

Electromagnetic energy harvesting depends on electrical currents which can be induced as the magnet arrives at the coil. This process is highly effective in environments characterized by vibrational or rotational motion in accordance with Faraday's law of electromagnetic induction. One design commonly shows a magnet that is attached to a spring and moves back and forth within a coil, the motion being that which creates the electrical output [5].

In devices wherein steady oscillation is observed, electromagnetic harvesters are chosen. For instance, In **Figure 1.2** dynamo lights when powered by the cycling motion of bikes or self-powered vibrational harvester retrofitting on industrial equipment to capture excess power. They can produce electric current for apparatus like wireless nanogenerators; thus, the device is appropriate for remote monitoring systems in abrasive conditions [6].

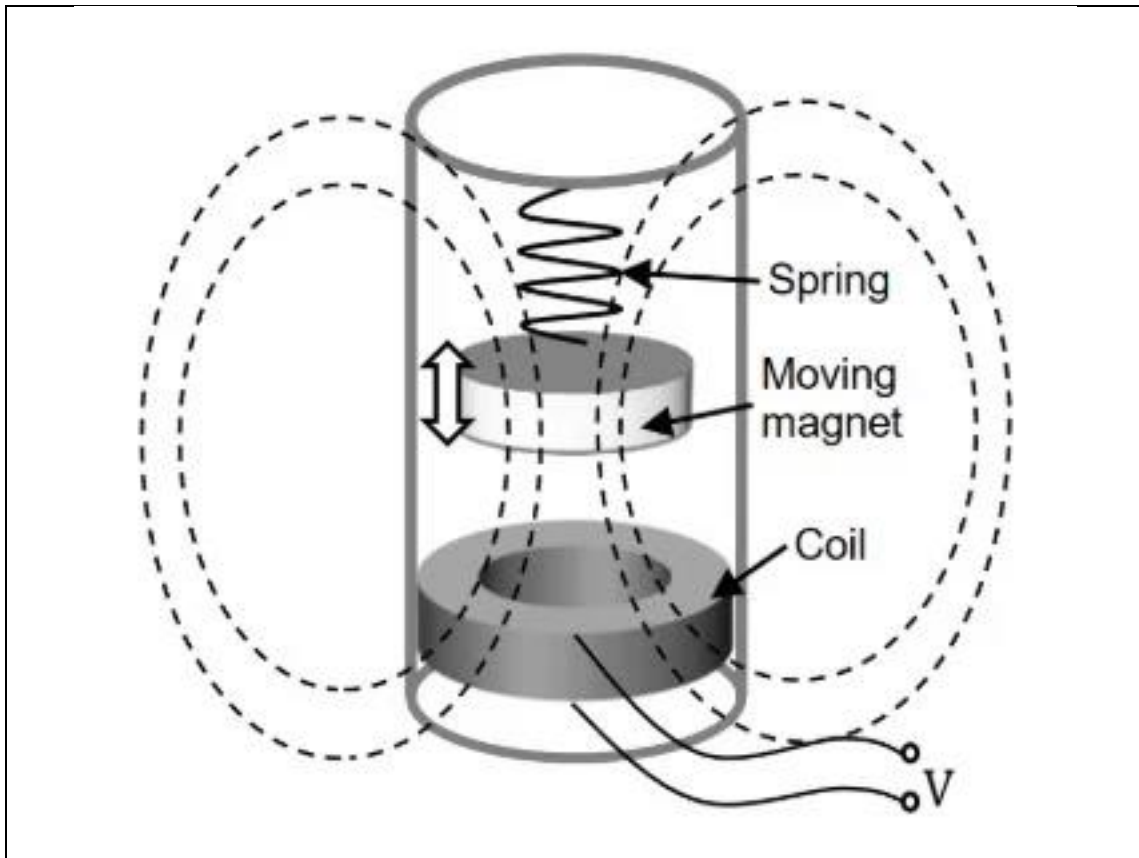


**Figure 1.2:** Schematic of Electromagnetic energy harvesting system[2].

### *1.2.3 Triboelectric Nanogenerators (TENGs)*

Triboelectric nanogenerators (TENGs) are newer to the class of mechanical energy harvesting devices. TENGs function on the mechanism of triboelectricity if one examines how two different materials produce charges of opposite polarity after contact and separation. These static charges are then converted to electric energy through the process called electrostatic induction.

In this paper, the TENG was described and designed based on the concept of triboelectric nanogenerators that was first developed by Prof. Zhong Lin Wang and his group in 2012. TENGs were at first intended for power acquisition from scaled-down motions like human movement and now have become one of the most prospective innovations in low-frequency mechanical energy harvesting. Building on the research of the Wang group, significant subsequent work has been done in this area, and TENGs have been used across numerous industries, including wearable technology and environmental monitoring, as well as large-scale energy generation from seashores[2, 7].

Unlike other energy harvesters dependent on high-frequency vibration, TENGs can supply power from low-frequency mechanical movement required in many applications making the device crucial for sustainable energy supply. For instance, TENGs operate in devices for motion tracking, environmental nanogenerators, and other large-scale ones including blue energy harvesting from ocean waves as shown in **Figure 1.3**.

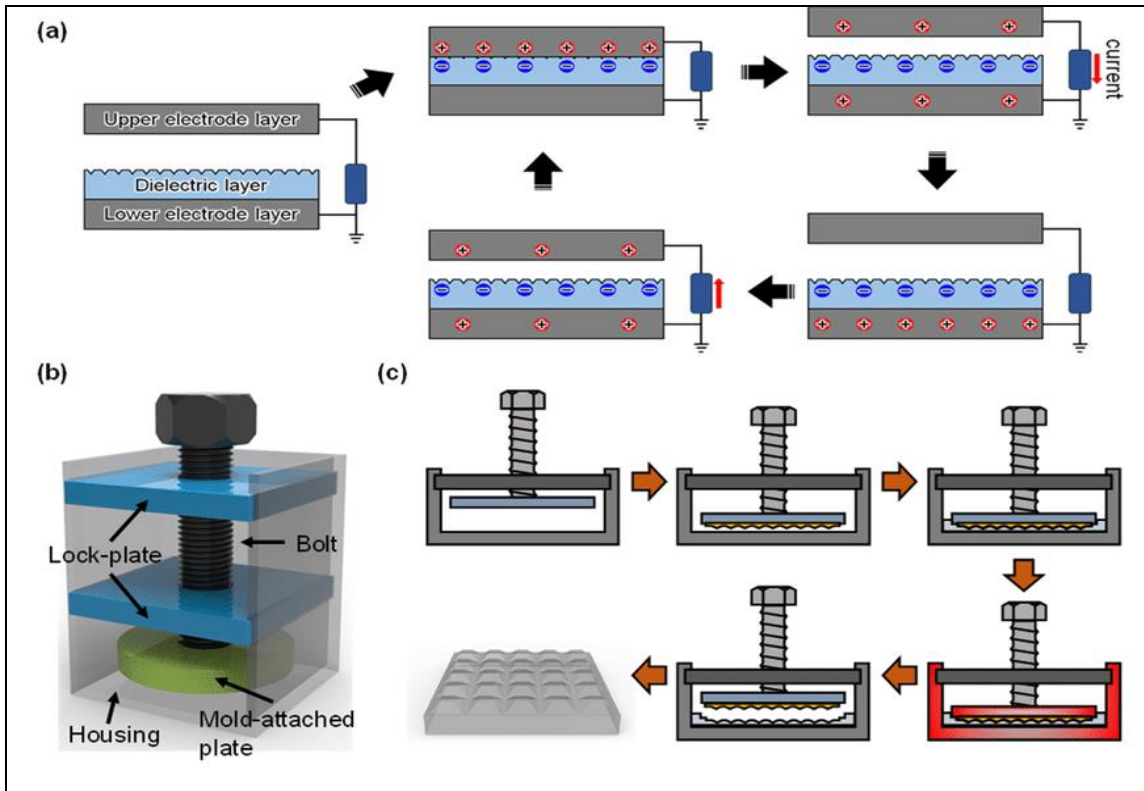


**Figure 1.3:** a) Dielectric energy harvesting schematic with charge separation between electrode layers. (b) Mold assembly setup with lock-plate, bolt, and mold-attached plate. (c) Stepwise mold fabrication process for the dielectric layer [3].

### 1.3 Triboelectricity

The concept of triboelectricity dates back 2400 years, discovered when amber and cat's fur produced sparks upon contact, hence deriving its name from the Greek words "Tribo" meaning rub and "electron" meaning amber. When two materials come into contact, especially insulators like PDMS and Teflon, or even some conductors like copper and aluminum, their surface becomes oppositely charged—a phenomenon known as the triboelectricity effect. This effect is not confined to solid interactions but also occurs in interactions between solids and liquids or gases. Triboelectrification is observed in daily life, such as feeling a spark when touching certain materials or witnessing a piece of paper stick to a balloon after rubbing it on hair [8]. Natural occurrences like lightning during thunderstorms, caused by colliding hailstones generating static charges that discharged as electric sparks, exemplify this effect. Similarly, during sandstorms, the

scattering of particles produces electrostatic charges, while volcanic eruptions generate sparks due to ash particulates colliding, leading to triboelectrification [9].

### *1.3.1 Triboelectric Series*

The choice of materials for fabricating triboelectric nanogenerator (TENG) devices is extensive, as any material can exhibit the triboelectric effect. The concept of a triboelectric series was first introduced by John Carl Wilcke in 1757, categorizing materials based on their electron affinity- how readily they lose or gain electrons. This series, illustrated in the below figure, arranges materials from positively charged near the top to negatively charged near the bottom, determined through contact electrification studies. Materials farther apart in the series exhibit more efficient charge transfer [10]: when a material at the bottom contacts one at the top, it acquires a negative charge. The effectiveness of the triboelectric effect also depends on the surface morphology of the materials, involving pyramids, needles, semi-circles, and cubes like surface morphology which enhance the contact area and triboelectrification. These morphologies can be implemented techniques like lithography, chemical etching, or laser ablation. Surface functionalization with molecules and nanoparticles further enhances surface potential and affects material properties. Composite materials, such as those incorporating piezoelectric nanoparticle in matrix, or making multi-layered structure composite can increase electrical output and permittivity, enhancing overall performance. The triboelectric series shown in **Figure 1.4**.

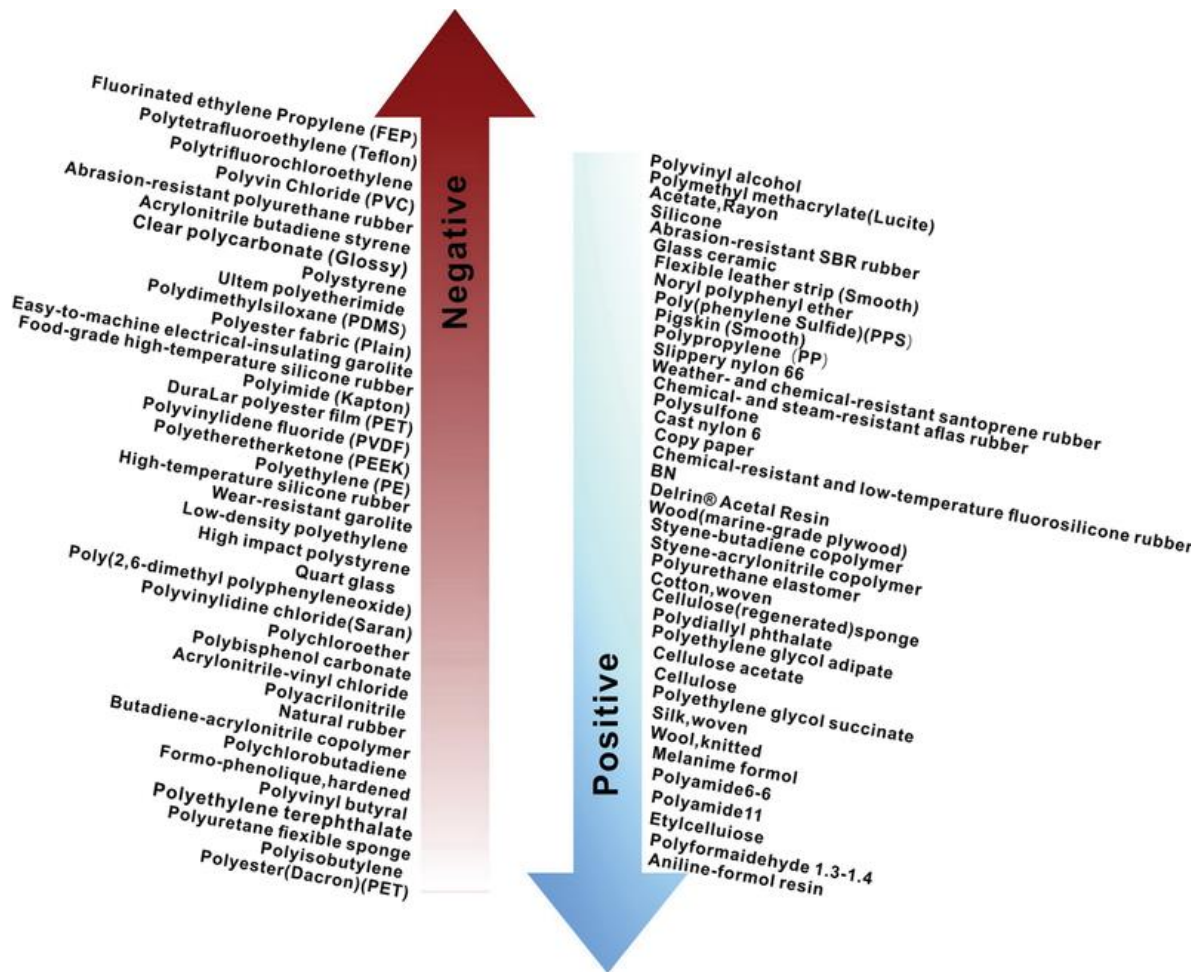


Figure 1.4: Schematic of Triboelectric series[4]

### 1.3.2 Theory of Triboelectricity

Despite its ubiquitous presence in daily life, the theoretical underpinning of the triboelectric effect remains elusive despite extensive research on the triboelectric series. Engineers, physicist, and chemists have all attempted to comprehensively study this phenomenon, yet uncertainties persist three primary mechanisms have been widely discussed as potential explanation [7]

#### 1.3.2.1 Electron Transfer

This mechanism primarily applies to conductors and involves the exchange of electrons due to differences in work functions. the work function, denoted as “ $\Phi$ ,” is an intrinsic

property of a material, representing the minimum energy needed to pull an electron from the solid. When two metals with different work functions come into-contact, a potential difference “ $V_C$ ” is established between their surfaces. This potential difference causes electrons to tunnel from one material to the other until equilibrium is restored.

$$V_C = \frac{\Phi_2 - \Phi_1}{e}$$

Harper figured that the total charge transferred during this phenomenon can be calculated by considering it as a parallel plate capacitor. Charge transferred “ $Q$ ” can be obtained by the equation:

$$Q = C * V_C$$

Where  $C$  is the capacitance of the system and  $V_C$  is the potential difference between the surfaces. This model helps in understanding the charging transfer dynamics during the contact electrification.

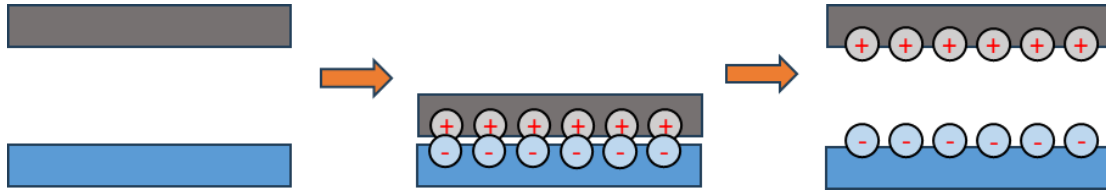


**Figure 1.5:** Schematic of Electron Transfer in TENG

Triboelectrification begins when two surfaces come into contact, initiating the transfer of charge. As the surfaces separate, electron tunneling ceases once a critical separation distance is reached, illustrated in **Figure 1.5**. Thus, electron transfer between metals is the main mechanism that explains triboelectrification [7].

However, this explanation, based on work function differences, does not extend to interactions between metals and insulators or between insulators themselves, due to the large band gap in insulators which impedes electron transfer. When two insulators ( $I_1$  and



$I_2$ ) come into contact, electrons from the valence band of  $I_1$  insulator cannot transfer to the conduction or valence band of the  $I_2$  because the valence states of  $I_2$  are already filled.

To address this, researchers proposed the surface state theory, which asserts that insulator surfaces have distinct surface state levels and work functions, facilitating electron transfer within these states. Fabish and Duke later, introducing the concept of acceptor and donor states for insulators, nevertheless, these theories lack robust experimental validation and remain unproven.

### 1.3.2.2 Ion Transfer

During the mid-20th century, electrophotography researchers discovered that polymeric toners with ionomers or molecular salts possess ions on their surfaces. Some of these ions are mobile, while others are immobile or loosely bound with opposite polarities. When two such insulators come into contact, mobile ions can transfer between them, leading to the generation of triboelectric charges, as illustrated in **Figure 1.6**.

The ion transfer mechanism primarily applies to ionic polymers because they can host mobile ions. Non-ionic polymers, on the other hand, are unable to facilitate this process due to their lack of mobile ions. However, it has been proposed that hydroxide ion on the surface of polymers might enable ion exchange in non-ionic polymers [7].

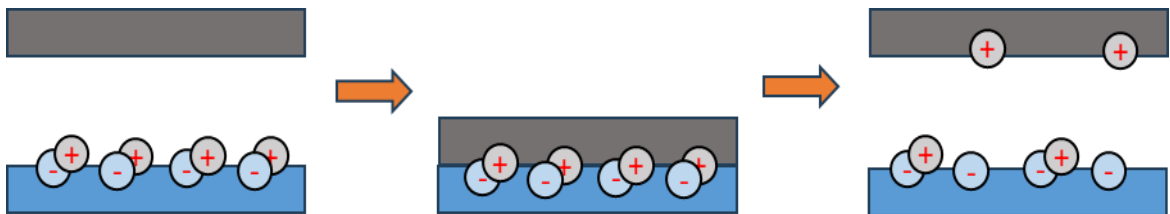


**Figure 1.6:** Schematic of ion Transfer in TENG

In contrast, Baytekin's experiments indicate that the water is not essential for triboelectrification,

Although it can stabilize surface charges. This finding suggests that while ion exchange may contribute to triboelectrification, it may not be the sole cause.

### 1.3.2.3 Material Transfer

This theory proposes that when two surfaces are rubbed against each other, microscale fragments of material are transferred from one surface to the other due to friction. These transfers particles carry charges, either from bond-breaking or surface contamination, as illustrated in **Figure 1.7**. However, this theory is considered flawed because triboelectrification is a highly reproducible process, and the material transfer should diminish with repeated contact [7].



**Figure 1.7:** Schematic of Material Transfer in TENG.

In 2011, Baytekin conducted experiments to test this theory, ultimately disproving the idea that opposite polarities consistently form on the surfaces. Instead, he suggested that the distribution of charges on the surfaces creates a mosaic pattern, resulting in net positive and negative charge distribution. Additionally, he used X-ray photoelectron spectroscopy, which revealed that both material and charge transfer occur during triboelectrification, this suggests that while material transfer might play a role, it is not the sole factor in triboelectrification.

## 1.4 Operational Modes of TENG

Triboelectric Nanogenerators (TENGs) are systems designed to transform mechanical energy into electrical power. They are used for energy harvesting and other applications, such as motion monitoring and self-powered nanogenerators, at both micro and macro scales. Depending on the application, TENGs can operate in various modes, including configurations with freely moving structures. There are four primary operation modes for TENGs, each tailored to specific requirements and application. These modes are explained in detail below.

### *1.4.1 Contact Separation Mode*

The contact separation mode was the first operational mode introduced for TENGs and is considered the most fundamental. This mode features a sandwich-like structure composed of two layers of dielectric material attached to electrodes, as illustrated in figure below. The mechanism works as follows: an external mechanical force brings one dielectric into contact with another, generating charges on their surfaces. When the dielectric is slightly separated, a potential difference is created between the electrodes connected to the dielectric layers.

The electrodes are externally connected to a load, causing electrons to flow from the negatively charged surface to the positively charged surface to balance the electrostatic field. This phenomenon is known as electrostatic induction. When the dielectric layer makes contact again, the electrostatic potential is reduced and eventually disappears at full contact as electrons flow back. Repeating this process generates an alternating current through the external load [11].

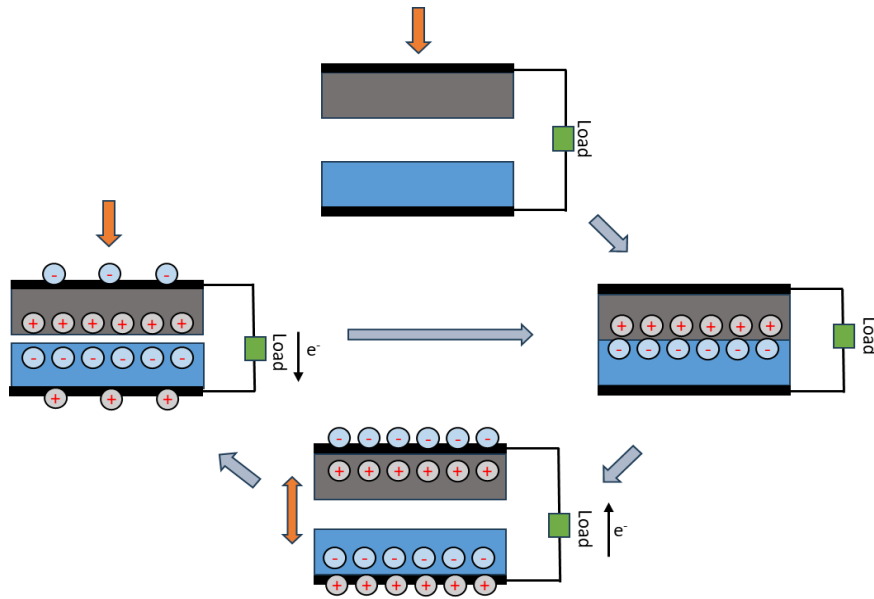


**Figure 1.8:** Schematic of Contact Separation Mode

Triboelectrification does not just occur between two insulating materials—it can also happen between an insulator and a conductor. This flexibility means that TENGs can be designed using either two dielectric layers or a combination of a dielectric and a conductor. Among the different TENG modes, the contact-separation mode stands out for its simplicity. It features a straightforward design with dielectric layers, electrodes, and a small separation gap arranged in a sandwich-like structure, as illustrated in **Figure 1.8**.

#### *1.4.2 Lateral Sliding Mode*

In the sliding mode of TENG, two distinct materials generate triboelectric charges on their surfaces as they slide against each other horizontally. When these materials separate after sliding, a potential difference is induced between the attached electrodes. This causes electrons to flow to balance the charge distribution, creating an electric current. The sliding mode is particularly useful for capturing energy from linear or rotational motions, due to its continuous contact and sliding mechanism. This mode can

utilize various combinations of dielectric and conductive materials for efficient energy harvesting [12].

#### *1.4.3 Single Electrode Mode*

The single electrode mode reduces the complexity of the TENG structure in order that an active triboelectric layer attached to an electrode, and the other counterpart can be any surface in the surrounding. Used on frictional contact, the charges selectively shift between the two objects due to triboelectric effect. On the separation of the materials, electrostatic induction results in flow of electrons between the single electrode connected to an electrical circuit and the other electrode which is in touch with the ground that provides an electrical output. This mode is flexible and efficient since energy could be harvested without having to directly bond a second electrode to the interacting material [13].

#### *1.4.4 Free-Standing Electrode Mode*

The free-standing electrode mode is one where a dielectric layer floats above the top electrode without being in physical contact with it. When the dielectric is shifting, the formation of the displacement results in a potential difference between the electrodes through tribo charges. This makes electrons move across the electrodes via a circuit external to the cell. This mode is very general, as the freely moving dielectric can be used in devices for motion sensing and in large-scale energy collection [14].

### **1.5 Problem Statement**

While triboelectric nanogenerators demonstrate potential as durable energy harvesters, several obstacles currently preclude their broad implementation. Chief among these is TENGs' inadequate conversion efficiencies, instability over time, and challenges mass-producing them cost-effectively. Addressing these limitations is imperative to make TENGs a viable alternative across diverse industrial uses. Further, their outputs fluctuate unpredictably depending on environmental conditions, questioning their dependability for steady energy collection in real-world situations.

Fundamentally, the low surface charge density of triboelectric materials limits the maximum power output of TENGs. However, with advanced materials engineering and design, these performance limitations can be encountered, overcoming a key challenge to scaling up their sustainable energy potential. A promising solution to address this issue involves incorporating Layered Double Hydroxides as a templating layer atop Polydimethylsiloxane to augment its triboelectric output. Known for its flexibility, chemical inertness, and strongly negative triboelectric effect, PDMS provides a steady baseline. Meanwhile, LDHs' tunable chemistry and charge-holding capacity furnish an adaptive coating that densifies surface charges. By depositing LDHs over PDMS, interfacial area expands, amplifying contact electrification. This not only heightens energy conversion efficiency but stabilizes triboelectric nanogenerator performance against environmental fluctuations. Another advantage is the ability to finely tune the LDH architecture for specialized needs, whether maximizing power density or tailored responses. Overall, the marriage of LDHs and PDMS presents a robust and customizable approach to triboelectric nanotechnology challenges.

In this research, LDHs serve as a surface template to augment the triboelectric effect of PDMS, resulting in a more efficient energy harvesting system. The combination of these materials creates a synergistic effect, improving the output voltage and current while maintaining flexibility and durability. This approach offers a scalable, low-cost solution for developing TENGs with higher energy conversion rates, making them suitable for a wide range of applications, from wearable technologies to large-scale environmental energy harvesting systems.

## 1.6 Choice of Materials

The properties of the materials used in triboelectric sensors are very important since it determines how the device will perform. It has been selected because of the following reasons that make it suitable to be incorporated in triboelectric sensors.

### 1.6.1 ZnAl-LDH

- ZnAl-LDH is particularly suitable for triboelectric nanogenerators based on the following factors. The basic structure of this compound is layered double hydroxide that has a larger surface area that is more desirable in improving the triboelectric effect. As the contact area between the triboelectric layers increases there is a direct relationship with the level of charges produced, which leads to an improvement in energy conversion efficiency. In terms of electrical properties, ZnAl-LDH exhibits satisfactory performance in charge transfer and storage to enhance the output performance of triboelectric nanogenerators (TENGs) [15].
- ZnAl-LDH is also very appreciated for its chemical and thermal stability and thus it is alkaline and able to preserve good efficiency in different conditions such as temperature and humidity. Ric effect. The larger the contact area between the triboelectric layers, the greater the charge generation, resulting in higher energy conversion efficiency. ZnAl-LDH also boasts favorable electrical properties, ensuring efficient charge transfer and storage, improving the overall output performance of triboelectric nanogenerators (TENGs) [15].
- ZnAl-LDH is also highly valued for its chemical and thermal stability, meaning it can maintain consistent performance under varying environmental conditions, such as fluctuating temperatures and humidity levels. In addition, it is a green material that fosters an environmentally sustainable society, as there is a growing concern in the proliferation of toxic free technologies. The ability to alloy it with other materials makes it easy to optimize it for use in particular applications, making ZnAl-LDH one of the most convenient materials to use in triboelectric nanogenerators [15].

### *1.6.2 MgAl-LDH*

- Likewise, MgAl-LDH is another suitable candidate for triboelectric applications, mainly because of the layer structure and the large surface area associated with the material. As in the case of ZnAl-LDH, the large flat surface area leads to increased charge creation through improved contact electrification. First, the application of MgAl-LDH in wearable and flexible electronics could benefit from the relative lightness of the material as compared to other types of electrodes [16].
- Also, MgAl-LDH possesses high dielectric constant below 10 nm essential for energy storage and conversion in enhancing the performance of TENGs [16].

### *1.6.3 PDMS Stacking on LDH*

- Polydimethylsiloxane (PDMS) is an essential layer in the TENGs' fabrication, especially for combined systems with LDHs. PDMS is often selected due to its high flexibility and mechanical strength, good electrical insulation, and outstanding triboelectric characteristics. When PDMS is located on top of LDH materials such as ZnAl-LDH or MgAl-LDH, it becomes an archetypal triboelectric couple because it has higher electronegativity than the LDH materials which makes it the electronegative layer while the LDH is the electropositive layer.
- The flexibility of the PDMS makes it easy for this material to conform to the shape of the LDH, which will help to increase the contact area necessary for the efficient charge creation during the triboelectric process, Excellent triboelectric properties. When PDMS is stacked on top of LDH materials like ZnAl-LDH or MgAl-LDH, it forms an ideal triboelectric pair, as the PDMS acts as a highly electronegative layer, while the LDH serves as an electropositive counterpart [17].
- The soft and flexible nature of PDMS allows it to conform to the surface of the LDH, maximizing the contact area and, thus, increasing the efficiency of charge generation during triboelectric interactions. In addition, the predicted chemical stability and elasticity of the PDMS are noteworthy, which will be suitable for the



flexible and stretchable electronic devices. This biocompatibility makes it even more suitable for the fabrication of wearable and skin attachable nanogenerators.

- Furthermore, the ability to insulate the generated charges for a longer period makes PDMS have a better output performance compared to other devices. chosen primarily for its flexibility, durability, and excellent triboelectric properties. When PDMS is stacked on top of LDH materials like ZnAl-LDH or MgAl-LDH, it forms an ideal triboelectric pair, as the PDMS acts as a highly electronegative layer, while the LDH serves as an electropositive counterpart [17].
- The soft and flexible nature of PDMS allows it to conform to the surface of the LDH, maximizing the contact area and, thus, increasing the efficiency of charge generation during triboelectric interactions. PDMS also exhibits excellent chemical stability and elasticity, which makes it particularly well-suited for applications in flexible and stretchable electronics. Its biocompatibility further enhances its suitability for wearable and skin-contact nanogenerators [17].
- Moreover, PDMS's insulating properties help retain the generated charges for a longer duration, further improving the output performance of the device. The deposition of PDMS on LDH not only increases the triboelectric effect but also offers improved mechanical integrity to the nanogenerator to perform in recurring motion or environmental conditions [17].

The integration of ZnAl-LDH, MgAl-LDH and PDMS can be viewed as a source of a promising strategy for the fabrication of efficient TENGs. The Layered doubled hydroxide provides the high surface area, electrical characteristics, and stability of the structure, while the PDMS provides the flexible attributes, strong triboelectric performance, and high durability. Together, these features form a highly effective and optimized triboelectric nanogenerator structure; the mechanical energy that can be harvested can be used in various applications with focus on wearable/flexible electronics technology.

## 1.7 Aims and Objectives

In this work, the objective is to prepare ZnAl-LDH and MgAl-LDH and investigate their potential for use in TENG for NH. The specific objectives of the study are:

- **Synthesis of ZnAl-LDH and Mg-Al LDH** using the hydrothermal method.
- **Preparation of ZnAl-LDH and Mg-Al LDH films** through a sacrificial method during the hydrothermal process.
- **Fabricating of PDMS layer** on LDH Surface.
- **Characterization** of the synthesized ZnAl-LDH and Mg-Al LDH to evaluate its structural, chemical, and physical properties.
- **Fabrication and prototyping** of a triboelectric nano generator using the prepared LDH/PDMS film.
- **Testing the performance** of the triboelectric nano generator, including output measurement using an oscilloscope.
- **Compare results** of Pristine LDH and LDH/PDMS TENG

My expected outcomes include enhancing the surface area of PDMS by utilizing LDH as a template, which is both cost-effective and easily prepared. By incorporating LDH materials such as ZnAl-LDH and MgAl-LDH, I aim to optimize the efficiency of energy scavenging and improve the durability of triboelectric nanogenerators. The synergy between PDMS and LDH will result in a complementary approach that increases the versatility and performance of the nanogenerators in various applications.

## CHAPTER 2: LITERATURE REVIEW

### 2.1 History

With technological advancement, global energy demands increase, whereby the need to look for other forms of energy apart from the established fossil energy source increases as well. To overcome this challenge, Wang's group developed the first Triboelectric Nanogenerator (TENG) to the world in 2012. TENGs have shown great promise in harnessing mechanical energy from the environment—energy that would otherwise go to waste—and converting it into electrical power. These devices are highly adaptable, with applications ranging from healthcare to numerous other fields, due to their compact design and cost-effectiveness, to maximize the triboelectric effect, significant research efforts have focused on optimizing device structures, materials, and surface morphologies. The subsequent sections will explore the advancements and innovations in TENG technology.

A key material contributing to the efficiency of TENGs is Polydimethylsiloxane (PDMS). PDMS serves multiple roles in TENGs, primarily as a flexible substrate that enhances device durability and performance. Its unique triboelectric properties improve the energy conversion efficiency, enabling better interaction with other materials in the device. Additionally, the excellent mechanical flexibility of PDMS allows TENGs to be integrated into various surfaces, including wearable technologies and portable devices, further expanding their application range[5].

To maximize the triboelectric effect, significant research efforts have focused on optimizing device structures, materials, and surface morphologies. Innovations in the fabrication of PDMS composites and coatings have led to enhanced triboelectric performance, as the surface roughness and texture can be fine-tuned to create optimal conditions for charge generation. The subsequent sections will explore the advancements and innovations in TENG technology, highlighting how the integration of materials like PDMS is pushing the boundaries of energy harvesting applications.

Here is some research efforts focused on enhancing the efficiency of PDMS through various patterning processes. These processes involve creating micro- and nano-scale structures on the PDMS surface to optimize its triboelectric properties. By manipulating the surface morphology, researchers can significantly increase the contact area and improve charge generation. Additionally, specific pattern designs can enhance the alignment of molecular interactions, further boosting the material's performance in applications like Triboelectric Nanogenerators (TENGs). Such advancements not only elevate the efficiency of PDMS but also open new avenues for its use in innovative energy harvesting technologies.

### *2.1.1 Patterning PDMS by Lithography*

Lithography has become a crucial technique in the enhancement of triboelectric nanogenerators (TENGs) by enabling precise micro- and nanoscale patterning of polydimethylsiloxane (PDMS) surfaces. Surface modification of PDMS is key to improving TENG performance by increasing the contact area and enhancing the triboelectric effect.

Kim et al. [6] proposed a large-area nanopatterning method utilizing block copolymer lithography on a flexible gold-substrate. In their work, a 100 nm-thick layer of gold (Au) was deposited on Kapton film via thermal evaporation. After removing the block copolymer template, an Au nano-dot pattern was formed on the surface, which dramatically enhanced the TENG's output performance. The  $I_{SC}$  and  $V_{OC}$  generated by the nanopatterned Au were 82  $\mu\text{A}$  and 225 V, respectively, compared to 22  $\mu\text{A}$  and 55 V for flat Au. This increase was due to the larger effective contact area of the nanopatterned surface, which improved the output power density to 93.2  $\text{W}/\text{m}^2$ —an impressive 16-fold improvement after BCP nanopatterning.

Fen et al. [7] created thin-film PDMS with micro-patterned surfaces, featuring designs like lines, cubes, and pyramids, using photolithography techniques. This involved creating silicon wafer molds to imprint the desired patterns onto the PDMS. These micro-structured PDMS layers were then utilized as friction layers in TENG devices. When paired with ITO-coated PET substrates in a sandwich-like configuration, the patterned

PDMS significantly boosted the device's performance. Notably, the pyramid-patterned PDMS surface achieved an open-circuit voltage of up to 18 V and a current of 0.7  $\mu\text{A}$ , which was four times greater than the output of flat PDMS.

Zhang et al. [8] advanced this technique further by introducing dual-scale structures in a sandwich-shaped TENG, which consisted of a 450  $\mu\text{m}$  thick PDMS layer patterned with pyramids and V-shaped grooves. These patterns were fabricated using photolithography and KOH wet etching. The dual-scale structures improved the TENG's output to peak values of 465V and a current-density of 13.4A/cm<sup>2</sup>. Compared to flat PDMS, this structure enhanced voltage by 100% and current by 157%, demonstrating the significant advantage of dual-scale micro/nanostructures in improving TENG efficiency.

### *2.1.2 Patterning PDMS by Micro needling*

A novel approach has been introduced by Ping Zhang [9], who proposed a new type of triboelectric nanogenerator consisting of micro-rhombic patterned PDMS (MR-TENG). This method simplifies the production of micro-rhombic patterns, utilizing only a wire bar coater, which reduces fabrication complexity and cost. The MR-TENG demonstrates impressive performance metrics, achieving an open-circuit voltage of 81 V and a short-circuit current of 2.04  $\mu\text{A}$ . These values represent an enhancement of 2.7 and 2 times, respectively, compared to triboelectric nanogenerators using smooth PDMS (S-TENG).

Moreover, the MR-TENG is versatile; it can function as a self-powered motion sensor capable of recognizing human motion states. Additionally, it can be integrated with electronic devices to create a self-powered system, enabling the powering of small wearable devices such as LCD screens, watches, and temperature and humidity sensors. The advantages of MR-TENG include cost-effectiveness, simplicity in the fabrication process, environmental friendliness, and miniaturization, indicating significant practical value in the realm of self-powered wearable sensors.

### 2.1.3 Patterning PDMS by Sputtering

Sputtering is a highly efficient method for improving the performance of triboelectric nanogenerators (TENGs), which convert mechanical energy into electrical energy. The efficiency of TENGs largely depends on the contact area of the triboelectric materials. Tao Wang et al. [10] devised a straightforward approach to enhance this contact area by creating a wrinkled surface on polydimethylsiloxane (PDMS) using an RF-sputtered ZnO sacrificial layer. This modification significantly boosted the performance of the TENG compared to a similar device made with flat PDMS. The optimized device achieved an open-circuit voltage of 170 V, a short-circuit current of  $8.7 \times 10^{-7}$  and a pulse output power density of 189  $\mu\text{W}/\text{cm}^2$ . These values were much greater, respectively, than those of the flat PDMS-based device. This simple and effective technique could pave the way for advancing TENG applications in flexible and wearable electronics.

In a related study, Jie Wang et al. [11] reported a TENG that integrates ultra-flexible PDMS films with micro-pyramid structures and sputtered aluminum electrodes. This configuration enables the device to achieve highly conformal contact with the skin, facilitating self-powered detection of human body motions.

The TENG employs a flexible polyethylene terephthalate (PET) film as a spacer layer, allowing the sensor to operate in contact-separation mode. This design ensures effective coupling of triboelectrification and electrostatic induction, resulting in a highly efficient energy conversion mechanism. The controllable and uniform micro-structured PDMS film is fabricated using a micro-electro-mechanical system (MEMS) manufacturing process, which contributes to the device's excellent sensitivity and high output performance.

Key performance metrics of the developed TENG include the capability to convert mechanical energy into electric energy sufficient to light up 110 LEDs. The sensor exhibits a sensitivity of approx. 2.5 V/kPa, excellent linearity ( $R^2 = 0.99522$ ), and stability up to 30,000 cycles. These features highlight the TENG's potential in wearable

applications, particularly for monitoring joint movements through conformal attachment to human skin.

The ultraflexible and self-powered characteristics of this TENG-based sensor present significant advantages over traditional rigid battery-operated devices, making it a promising candidate for future advancements in wearable electronics.

#### *2.1.4 Patterning PDMS by Direct Laser*

Mechanical energy, abundant and ubiquitous in our daily lives, has significant potential for scavenging, making it a valuable resource for energy conversion. The triboelectric nanogenerator (TENG) has emerged as a promising solution for efficiently converting ambient mechanical energy into electrical energy. Among various materials used in TENGs, polydimethylsiloxane (PDMS) is commonly selected as a friction layer due to its superior mechanical and electrical properties.

Recent research by Daewon Kim et al. [12] has revealed a strong correlation between the output power of TENGs and the Young's modulus of PDMS. By optimizing the PDMS mixture ratio, enhancements in output power can be achieved. Furthermore, to further increase the output power of TENGs, a well-ordered microstructure can be created directly on the surface of PDMS using ultrafast laser irradiation. This direct patterning technique is more efficient than conventional surface modification methods, such as replication and other microfabrication steps.

The experimental results demonstrate that a TENG utilizing patterned PDMS with a laser power of 29 mW achieves more than double the output power compared to a control TENG using bare PDMS. Specifically, the TENG with the patterned PDMS reaches a maximum output power density of 107.3  $\mu\text{W}/\text{cm}^2$ . This innovative approach to direct laser patterning not only enhances the energy conversion efficiency of TENGs but also simplifies the fabrication process, paving the way for advanced applications in energy harvesting.

**Table 2.1:** Literature Comparison.

<b>METHOD</b>	<b>AUTHOR</b>	<b>TECHNIQUES DETAILS</b>	<b>PERFORMANCE METRICES</b>
<b>LITHOGRAPHY</b>	Kim et al. [6]	Utilizes block copolymer (BCP) lithography on flexible gold substrate.	$I_{sc}$ : 82 $\mu$ A, $V_{oc}$ : 225 V, Output power density: 93.2 W/m <sup>2</sup> (16-fold improvement).
	Fem et al. [7]	Developed thin film micropatterned PDMS using photolithography with features like lines, cubes, and pyramids.	Output voltage: 18 V, Current: 0.7 $\mu$ A (4 times higher than flat PDMS).
	Zhang et al. [8]	Introduced dual-scale structures using pyramids and V-shaped grooves via photolithography and KOH etching.	Output voltage: 465 V, Current density: 13.4 A/cm <sup>2</sup> (Voltage increase: 100%, Current increase: 157%).
<b>MICRO NEEDLING</b>	Ping Zhang et al. [9]	Proposed micro-rhombic patterned PDMS (MR-TENG) with wire bar coater for simple production.	Open-circuit voltage: 81 V, Short-circuit current: 2.04 $\mu$ A (2.7 and 2 times higher than smooth PDMS).
<b>SPUTTERING</b>	Tao Wang et al. [10]	Developed a method to wrinkle PDMS using rf-sputtered ZnO sacrificial layer.	VOC: 170 V, ISC: $8.7 \times 10^{-7}$ A, Output power density: 189 $\mu$ W/cm <sup>2</sup>
	Jie Wang et al. [11]	Integrated ultraflexible PDMS films with micro-pyramid structures and sputtered aluminum electrodes.	Sensitivity: 2.54 V/kPa, Operates in contact-separation mode, capable of lighting up 110 LEDs, Good stability (30,000 cycles).



<b>DIRECT LASER</b>	Daewon Kim et al. [12]	Created microstructures on PDMS via ultrafast laser irradiation for enhanced output power.	Max output power density: 107.3 $\mu\text{W}/\text{cm}^2$ (More than double the output power compared to flat PDMS).
---------------------	---------------------------	--	--

## 2.2 State of Art

Surface patterning of Polydimethylsiloxane (PDMS) has garnered significant attention due to its broad applications in areas such as energy harvesting, sensors, and biomedical devices. Numerous approaches have been developed to enhance the surface area of PDMS and improve its performance, particularly in Triboelectric Nanogenerators (TENGs). Common methods for patterning PDMS include lithography, micro-needling, sputtering, and direct laser patterning. These techniques have demonstrated success in increasing surface roughness and improving efficiency. However, they often come with challenges such as high costs, complex fabrication processes, and the need for specialized equipment.

In contrast, my research introduces a novel and more cost-effective approach by using Layered Double Hydroxides (LDHs) as a template for surface patterning. LDHs are readily available, easily synthesized, and nanostructured 2D material. By employing LDH as a template and coating it with PDMS, we can achieve a significant enhancement in surface area without the need for expensive or complicated processes. This approach not only preserves the porous, layered structure of LDH but also allows the PDMS to conform to and replicate the high-surface-area template, resulting in improved triboelectric and functional properties.

Compared to previously established methods like lithography, micro-needling, sputtering, or direct laser patterning, the use of LDH offers a simpler, scalable, and cost-effective solution for surface patterning of PDMS. This method maintains the high performance of patterned surfaces while reducing fabrication costs, making it a promising alternative for large-scale applications in energy harvesting and other fields.

## CHAPTER 3: MATERIAL AND METHODS

### 3.1 Synthesis Route

For the synthesis of Zinc-Aluminum Layered Double Hydroxide (ZnAl-LDH), the following methods were employed:

- **Hydrothermal Method:** This method was used to synthesis of ZnAl-LDH. Hydrothermal synthesis involves heating the precursor in an airtight vessel at elevated temperatures and pressures that are favorable for the formation of the layered double hydroxides [28].
- **Sacrificial Method:** The sacrificial method was used when preparing the ZnAl-LDH film. In this method a sacrificial layer is used to help form the ZnAl-LDH film and this layer is then dissolved to reveal the required film structure.
- **PDMS/LDH:** Deposition of PDMS on LDH through the curing of PDMS on the LDH surface using the coating trough a doctor blade.

### 3.2 Materials and Apparatus Required

- Zinc-nitrate-hexahydrate ( $\text{Zn}(\text{NO}_3)_2 \cdot 6\text{H}_2\text{O}$ )
- Magnesium-nitrate-hexahydrate ( $\text{Mg}(\text{NO}_3)_2 \cdot 6\text{H}_2\text{O}$ )
- PDMS (182 sylgard) silicon kit
- Hexamethylenetetramine (HMTA)
- Sodium Hydroxide (NaOH)
- Hydrochloric acid (37% HCl)
- Polydimethylsiloxane (PDMS)
- Ethanol
- Distilled water
- Kapton tape

- Kapton sheet
- Copper tape
- Aluminum tape
- Copper wires
- Double-sided tape
- Aluminum foil
- Acrylic
- Borosilicate glass reactor
- Drying oven
- Magnetic stirrer
- Hotplate
- Microscopic plates
- Beakers
- Petri dishes
- Weighing balance
- Fume hood
- Centrifuge
- Tweezer

### **3.3 Synthesis of ZnAl-LDH and MgAl-LDH**

In this work, LDH was prepared through hydrothermal growth in-situation. In this synthesis, Zinc Nitrate Hexahydrate ( $\text{Zn}(\text{NO}_3)_2 \cdot 6\text{H}_2\text{O}$ ) or Magnesium Nitrate Hexahydrate ( $\text{Mg}(\text{NO}_3)_2 \cdot 6\text{H}_2\text{O}$ ) were used ; both of which were purchased from Sigma-

Aldrich with a reported purity of 99%, alongside Hexamethylenetetramine (HMTA) both of which were obtained from Sigma-Aldrich with a purity of 99%. For synthesizing the precursor solution, 20 mmol of  $\text{Zn}(\text{NO}_3)_2 \cdot 6\text{H}_2\text{O}$  or  $(\text{Mg}(\text{NO}_3)_2 \cdot 6\text{H}_2\text{O})$  and 20 mmol of HMTA were stirred in 250 ml of DI water till all the solid completely dissolved. Aluminum substrate used in the trivalent is the source of trivalent and pretreatment was done by washing the substrate with 10% HCl, ethanol and DI water to remove impurity. The cleaned aluminum substrate was oriented at an angle of  $45^\circ$  to the base of the borosilicate glass reactor containing the above prepared precursor solution. This setup was moved to a forced convection oven and was heated at  $90^\circ\text{C}$  for 6 hours to promote the hydrothermal reaction which allows the growth of the ZnAl-LDH film. The orientation of the aluminum substrate was slanted to avoid the formation of large water bubbles that interfered with ion conduction and in addition, it supported the formation of a definite film structure. After the reaction, the substrate film consisting of ZnAl-LDH film was exposed to oven heat for 30 min at  $60^\circ\text{C}$  to eliminate deposited water on the samples. This procedure provided a well ordered ZnAl-LDH film that can be used for further operations and shown in **Figure 3.1**.

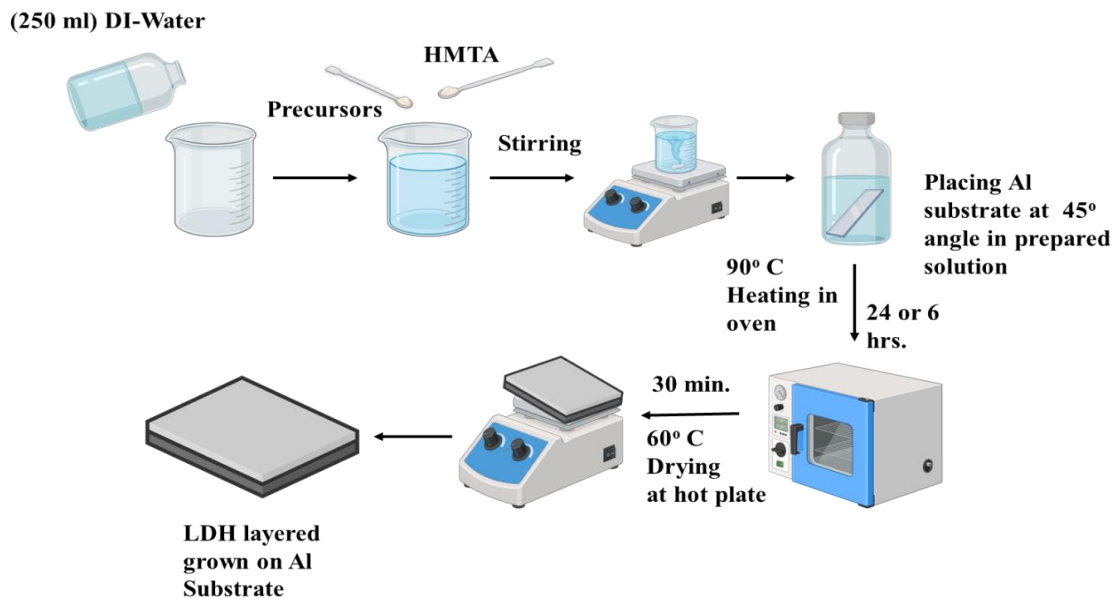


**Figure 3.1:** Schematic of LDH film preparation.

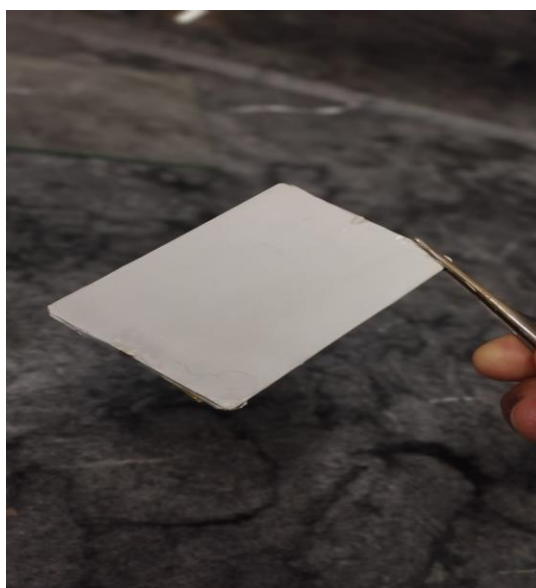


**Figure 3.2:** Digital image of LDH Film

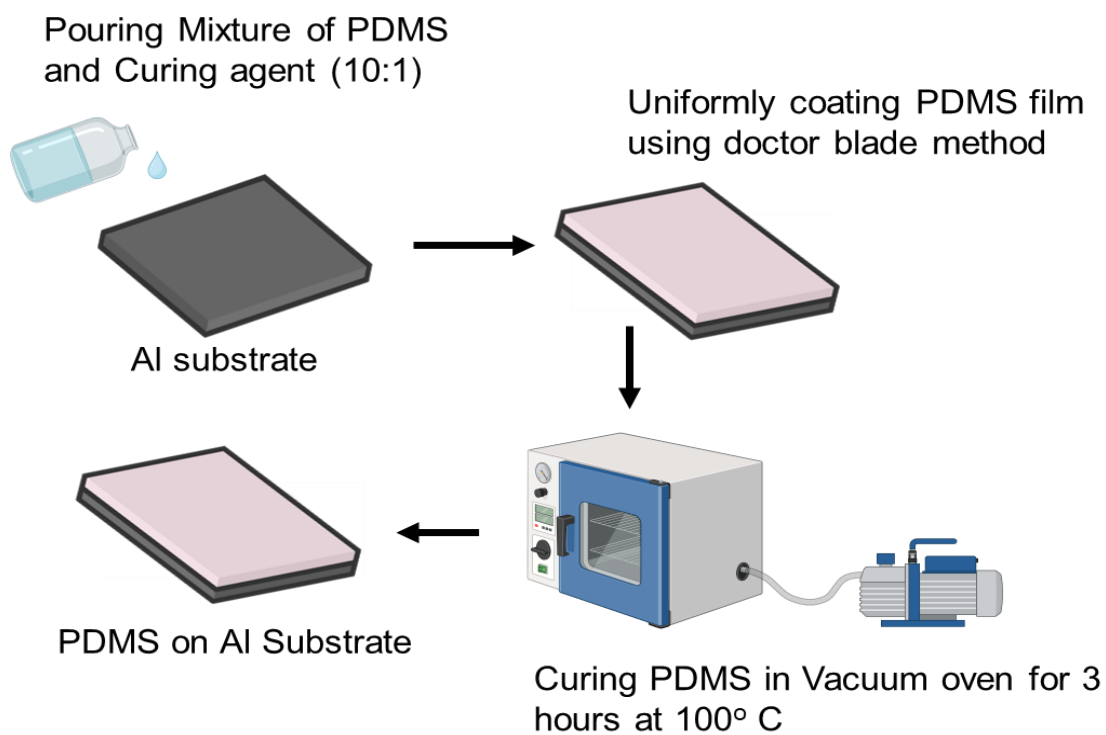


**Figure 3.3:** Schematic of PDMS stacking and curing on LDH film.

### 3.4 Fabrication of TENG

The fabrication of the triboelectric nanogenerators (TENGs) involves three different designs: PDMS-Al TENG, the LDH-PDMS TENG device, and the LDH/PDMS-Al TENG device. The active layer in the PDMS-Al TENG is made of polydimethylsiloxane (PDMS) material, while aluminum (Al) plate is the counter back electrode layer. In the LDH-PDMS TENG, the Zinc Aluminium Layered Double Hydroxide (ZnAl-LDH) is coated on one of the friction layers, and the other is polydimethylsiloxane (PDMS). The PDMS Fabrication steps shown in **Figure 3.3**. The LDH/PDMS-Al TENG has ZnAl-LDH as the friction layer and PDMS as the other friction-layer, whereas aluminum is the counter layer and back electrode. For all these designs, friction layers are provided on acrylic substrates, which are separated by arc-shaped Polyamide (PI) sheets for contact-separation functionality. Such an arrangement allows variations in the contact surfaces of the friction layers to maximize the triboelectric process and improve the performance of each TENG design.

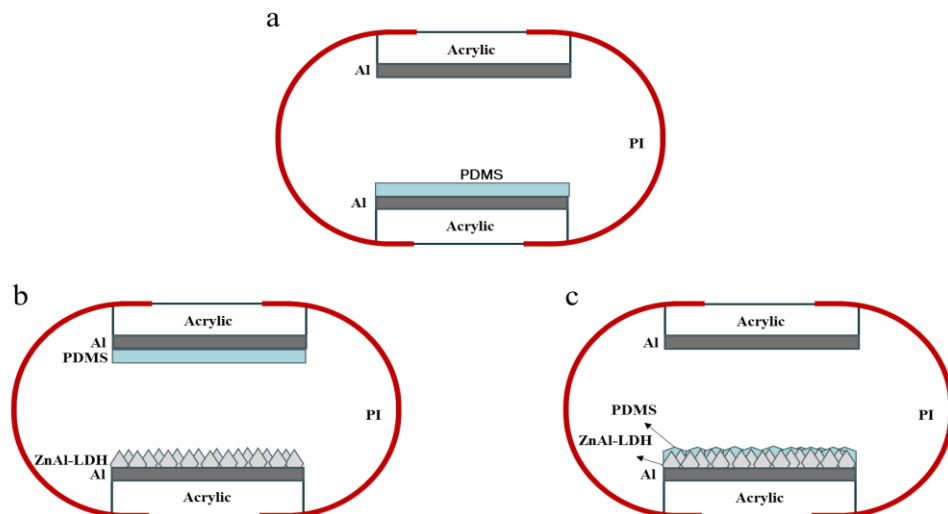


**Figure 3.4:** Prototyping and working mechanism of TENG device.

### 3.4 Characterization Techniques

#### 3.4.1 Scanning Electron Microscopy (SEM)

Sample Preparation (LDH Film): In this research a LDH film was synthesized and characterized by SEM. The patterns were imaged at magnifications between 1 micron and 10 microns to investigate surface features and topographic features. Furthermore, the Energy Dispersive Spectroscopy (EDS) test was conducted in conjunction with SEM to identify the proportional quantity of the constituents of the LDH film. The Scanning Electron Microscope system used is the model's name JSM 6490LA which is available in the SCME department of the School of Chemical and Materials Engineering NUST Islamabad.

#### 3.4.2 X-Ray Diffraction (XRD)

Sample preparation for XRD: The sample is prepared as in powder form and then placed in XRD STOE diffractometer at SCME-NUST with scan angle of 20–80° and scan rate is 5°/min and Cu source is used for X-ray source then the raw file is draw on origin to check the XRD diffractogram and match it with JCPDs card number of LHD based materials.

#### 3.4.3 Fourier Transform Infrared (FTIR)

Sample Preparation Example (Pellet Form): In this case to obtain the sample for the FTIR analysis, the LDH powder sample was prepared and packed to form pellet by incorporating with potassium bromide (KBr), which is standard method to prepare the samples for FTIR analysis [29]. The pellets were made with the help of hydraulic press at a pressure of 7 tons for 10 seconds. Lastly, the pellets were analyzed in the FTIR machine in the Surface Engineering Lab at SCME-NUST after preparation. This method enabled complete identification of the functional groups and bonds in the LDH material.

### 3.4.5 Digital Oscilloscope

Sample Preparation Example (TENG Device): For testing in this study, a triboelectric nanogenerator (TENG) device was fabricated. One terminal of the device in this case was grounded with a Layered Double Hydroxide (LDH) film while the other terminal was in contact with an aluminum electrode. The output voltage ( $V_{OC}$ ) and short circuit current ( $I_{SC}$ ) was recorded by RIGOL Digital Oscilloscope (DS1000E Series,) available in the RIMS Micro-Nano lab at NUST. To measure the current with greater precision, a two-stage amplifier circuit was used for amplification of the acquired signals to capture the detailed electrical behavior of TENG.

Specifications such as design, analysis and performance of the TENG device were discussed in the “Results and Discussion” section, to which the characterization techniques including XRD, FTIR, SEM, and digital oscilloscope made significant contributions. XRD analysis verified the crystalline nature of the LDH film and dominant functional groups for triboelectric functions were determined from FTIR analysis. By using SEM, the film surface topography that is critical in charge transfer processes was observed. Voltage measurements using the output voltage and using the digital oscilloscope established the short circuit current and two stage amplifiers analyzed the current properly. The synergetic outcomes of these individual experimental findings reveal the relationship between structural characteristics of the material and the electric power conversion efficiency.



## CHAPTER 4: RESULTS AND DISCUSSION

### 4.1 Materials Characterizations

The characterization and performance results of the synthesized ZnAl-LDH materials are presented fully herein and discussed thoroughly. In depth analysis of the data derived from XRD, FTIR, SEM and TENG performance evaluation used is discussed in the discussion. The morphological, structural, and electrochemical properties of the ZnAl-LDH materials as well as their effect on the triboelectric nanogenerator performance are clearly highlighted in each section. We interpret these key findings in light of relevant theoretical frameworks and compare them with prior literature for a comprehensive understanding of these results.

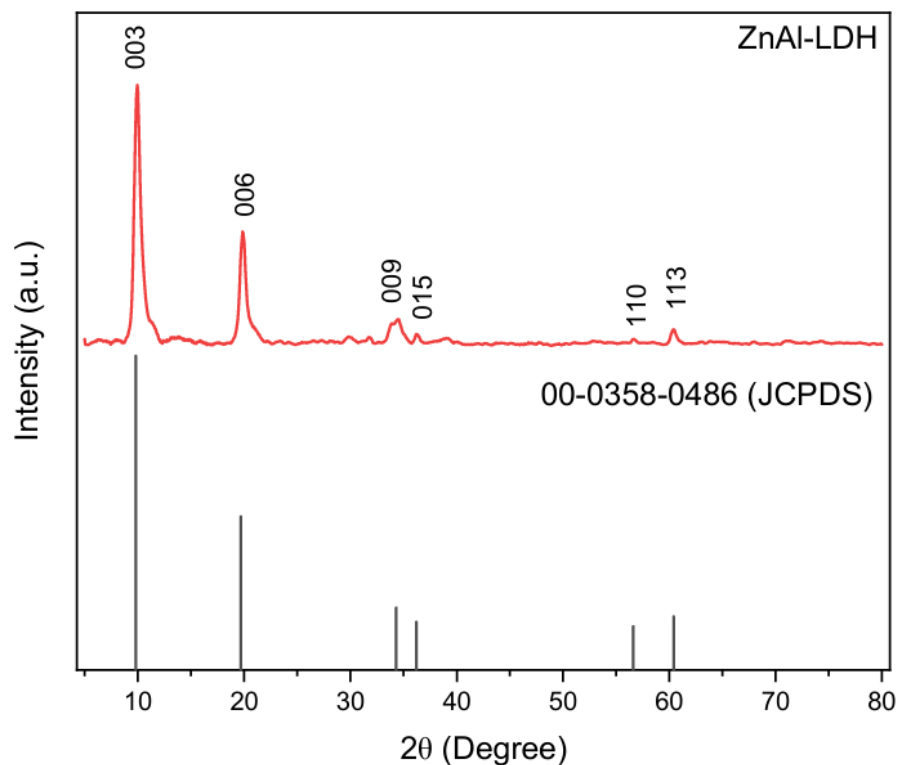


**Figure 4.1:** XRD diffractogram of ZnAl-LDH.

In **Figure 4.1** XRD Graph of ZnAl-LDH sample shows a strongly crystalline layered structure with the strongest peak at  $9.8^\circ$  corresponding to the (003) plane. reflections at  $34.3^\circ$  (009) and  $19.7^\circ$  (006) confirm the LDH layer layers stack regularly and, strong ordering along c axis. These basal reflections show that the material contains well-ordered layers with minimal defects.

Furthermore, the peaks at higher angles,  $56.6^\circ$  (110) and  $60.4^\circ$  (113), are at in-plane metal-metal distances within the hydroxide layers and hence demonstrate that ZnAl-LDH has a brucite-like structure. High crystallinity is indicated by the sharpness and intensity of these peaks, implying successful synthesis of a well-ordered material. Ordered and crystalline structures which facilitate the materials' potential applications in catalysis and energy storage are desired.

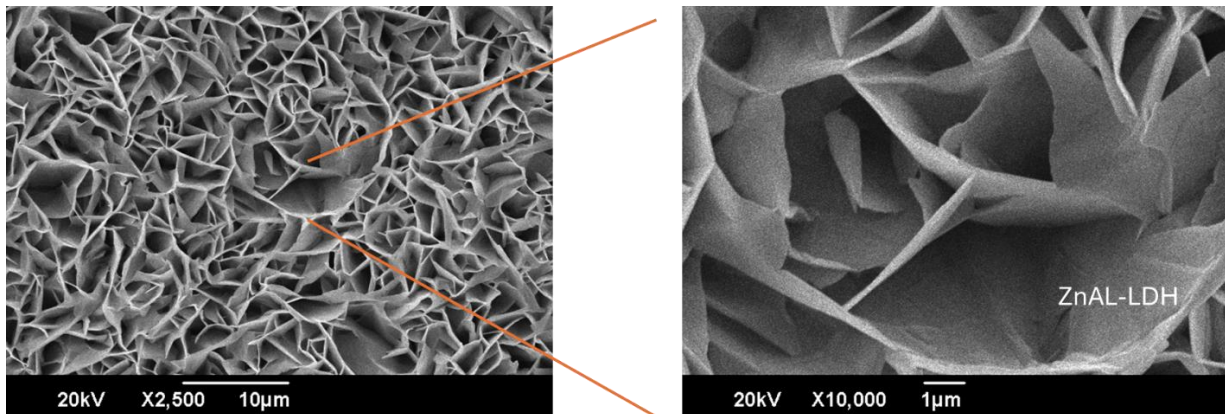


**Figure 4.2:** SEM images as synthesized ZnAl-LDH.

In **Figure 4.2** the SEM images of as synthesized ZnAl-LDH show a porous, layered-structure composed of crumpled nanosheets. At lower magnification (X2500), the material appears densely packed, forming an interconnected network of wrinkled layers, which increases surface area. At higher magnification (X10,000), the thin, folded sheets are more distinct, highlighting the layered double hydroxide's characteristic morphology. This structure is crucial for applications requiring high surface area, such as energy storage or catalysis, where increased surface interaction enhances performance.

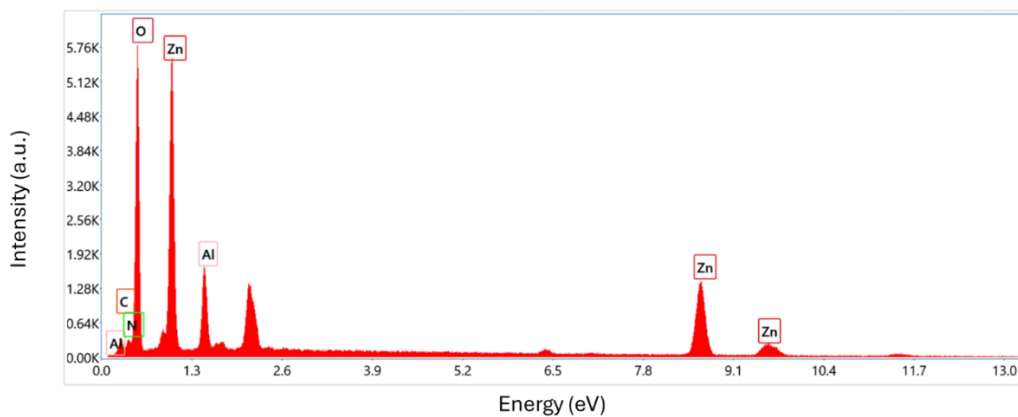


**Figure 4.3:** EDS of ZnAl-LDH.

In **Figure 4.3** the quantitative elemental composition of the material is obtained from the EDS spectrum. Oxygen (55.2%), Carbon (22.3%), Zinc (11.4%), Nitrogen (6.7%), Aluminum (4.4%) are the main elements detected. The combination of high oxygen content and the presence of Zinc and Aluminum lends credence to the fact that this material contains metal oxides (ZnO and Al<sub>2</sub>O<sub>3</sub>) present to provide its structural integrity and possible catalytic properties. Evidence of some organic or carbonaceous material is indicated by the huge carbon presence, and the material may function better in several applications.

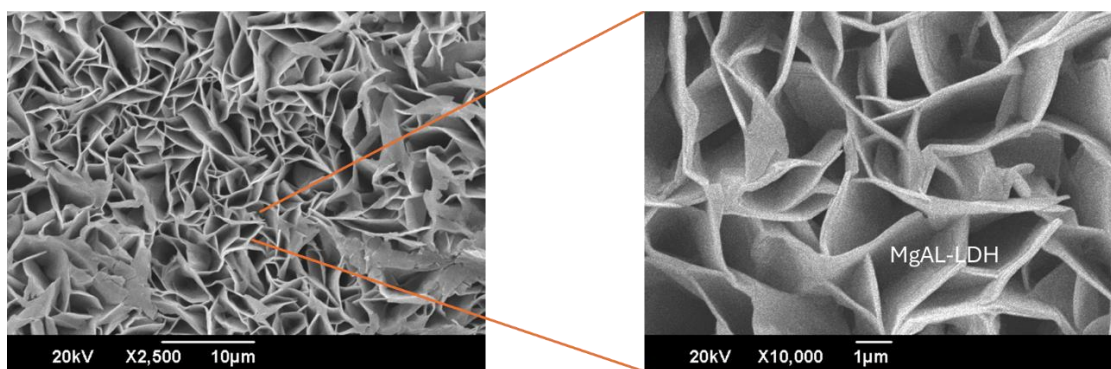


**Figure 4.4:** SEM images of MgAl-LDH.

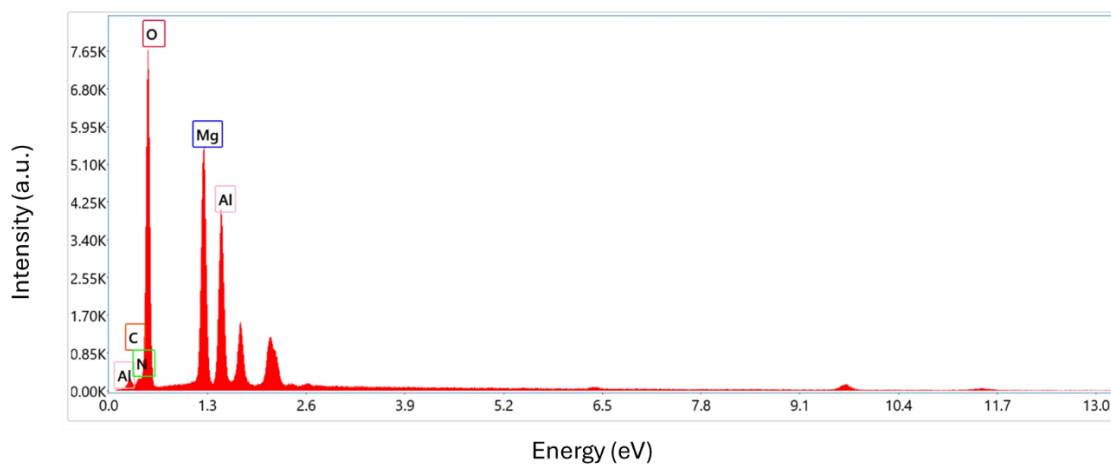


**Figure 4.5:** EDS of MgAl-LDH.

In **Figure 4.4** SEM images of MgAl-LDH show a porous, layered structure like ZnAl-LDH, composed of crumpled nanosheets. At lower magnification (X2,500), the material displays a densely packed, interconnected network of wrinkled layers, enhancing the surface area. At higher magnification (X10,000), the thin, folded nanosheets are clearly visible, further emphasizing the characteristic morphology of layered double hydroxides. This structure is essential for applications requiring high surface area and active interaction, such as in catalysis or energy storage, where these features improve performance.

In **Figure 4.5** shows that the material is primarily Oxygen (59.3%) with 15.7% Carbon, 11.7% Magnesium, 8.3% Aluminum, and 5.1% Nitrogen. The metal oxides presumably are present and their presence is suggested by the high oxygen content and by the presence of magnesium and aluminum. The catalytic activity and structural stability of oxides in these materials are important. The presence of some organic or carbonaceous components are indicated by the carbon and nitrogen content, which will increase the overall property of the material with respect to some applications.

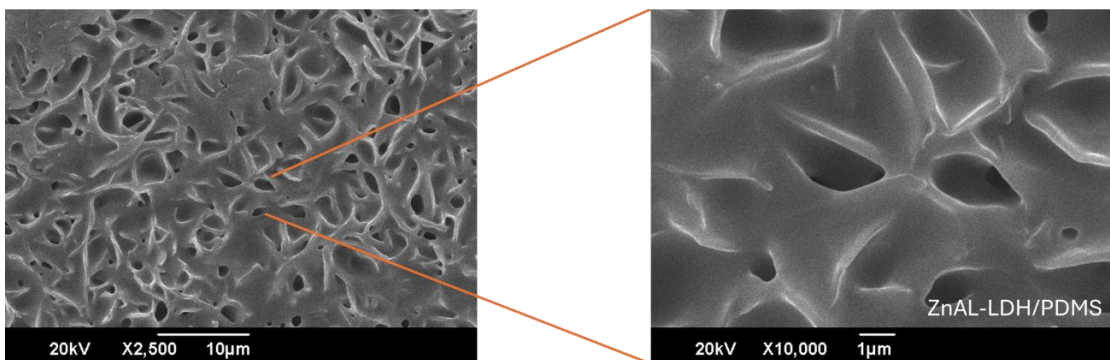


**Figure 4.6:** SEM images of PDMS stack on LDH surface.

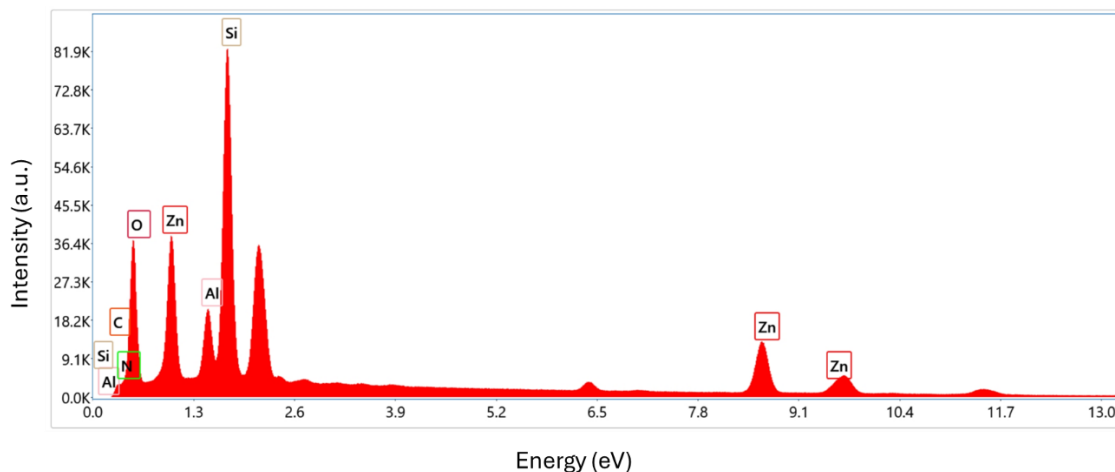


**Figure 4.7:** EDS of PDMS/ZnAl-LDH sample.

In **Figure 4.6** the left side image displays the porous material at  $\times 2,500$  magnification, revealing a highly porous structure with interconnected pores spread across the surface. These pores are characteristic of the layered double hydroxide (LDH) structure and are further enhanced by the PDMS coating, which conforms to the surface topology, preserving and enhancing the porosity. This porous architecture increases the material's surface area, enabling more potential sites for interactions in catalysis, gas sensing, and adsorption.

The right-side image is a zoomed-in view of the left side at  $\times 10,000$  magnification, highlighting the layered and crumpled morphology of the ZnAl-LDH. The PDMS coating spreads uniformly over these layers without blocking the pore structure, improving surface effects while maintaining the inherent porous structure of the material. This results in an increased surface area, with the PDMS covering the surface and penetrating the pores, enhancing both the total surface area and the functional efficiency of the material sample.

In **Figure 4.7** the elemental composition of the ZnAl-LDH sample coated with PDMS is confirmed by the EDS spectrum shown in Fig. 2. They were detecting Gaussian peaks with oxygen (47.6%), silicon (17.5%), nitrogen (10.9%), carbon (10.4%), zinc (9.0%) and aluminum (4.6%). The high amount of oxygen content and the presence of silicon and carbon verify that the structure of PDMS is integrated to the LDH. The high Oxygen content is also related to the high content of metal oxides in the material, and the

Silicon content proves the presence of the PDMS layer responsible for inducing the surface properties of the material.

Finally, the addition of a PDMS coating to the surface of ZnAl-LDH significantly improves surface area without altering the porous structure of the LDH and allows for the addition of the flexibility and surface enhancing properties of PDMS. For applications in which performance relies on a high surface area, this combination makes the material uniquely suitable.

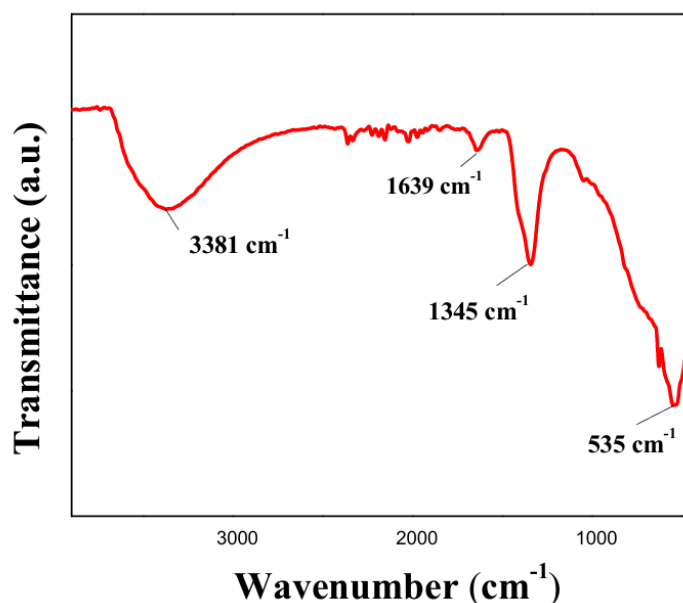


**Figure 4.8:** FTIR graph of ZnAl-LDH.

In **Figure 4.8** the FTIR spectrum graph for the ZnAl-LDH sample includes absorption bands that are characteristic of the functional groups and molecular bonds present with the material.

1. Broad Absorption Band at  $\sim 3500\text{ cm}^{-1}$ : The broad peak corresponds to that of the stretching vibrations of hydroxyl groups (-OH). It is likely, these hydroxyl groups are resulting from interlayer water molecules and hydrogen bonding within the LDH structure. Typical features of LDH materials are the presence of water in the layered structures, most often intercalated between the crystal layers.

2. Absorption around  $\sim 1600\text{ cm}^{-1}$ : The water molecular bending mode (H-O-H bending) peak is located at  $1600\text{ cm}^{-1}$ . Finally, the presence of interlayer water in the

ZnAl-LDH sample is further confirmation of these molecules being typically held within the interlayers of LDH structures.

3. Peak at  $\sim 1380\text{ cm}^{-1}$ : As can be seen this absorption band indicates presence of nitrate ions ( $\text{NO}_3^-$ ) in the structure. However, since nitrate salts were used during synthesis, the  $\text{NO}_3^-$  anions could be intercalated as charge balancing ions between the layers of the ZnAl-LDH. The incorporation is also successfully confirmed for nitrate anions into the LDH structure.

4. Bands around  $\sim 700\text{-}900\text{ cm}^{-1}$ : The assignment of these bands are typically Metal-O and Metal-OH vibrations (Metal = Zn, Al). They are the metal oxygen bonds through the LDH structure, with zinc and aluminum in the brucite like LDH layers. These bands confirm successful formation of the ZnAl-LDH material and characteristic mixing of the metal ions within the layered structure.

5. Low-frequency Bands ( $<700\text{ cm}^{-1}$ ): ZnAl LDH is further shown to incorporate metal-oxygen bonds in zones beyond the low-frequency bands associated with interlayer spacing modes, and in additional low-frequency bands associated with Zn-O and Al-O bonds. These are characteristics of layered hydroxides, and additional evidence of a characteristic layered double hydroxide structure.

In conclusion FTIR spectrum shows that ZnAl-LDH has been successfully synthesized with clear hydroxyl and metal oxygen, water, and nitrate peaks. The associated spectrum is consistent with expected functional groups and structural building components of LDH materials and suggests that the material was prepared as intended with interlayer water and nitrate anion.



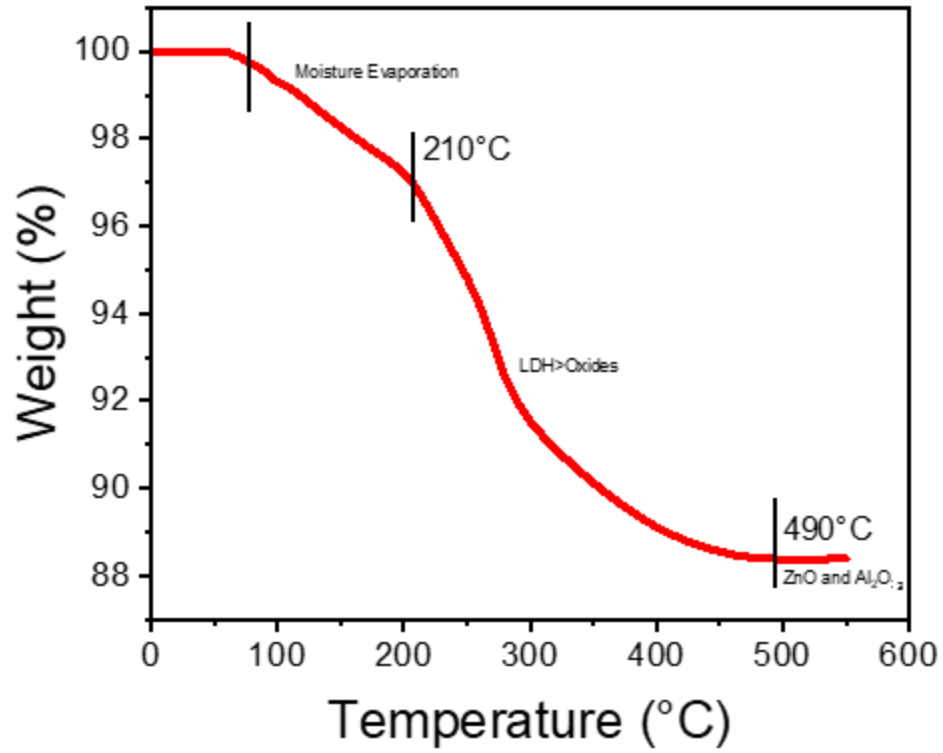


Figure 4.9: TGA Graph of pristine ZnAl-LDH.

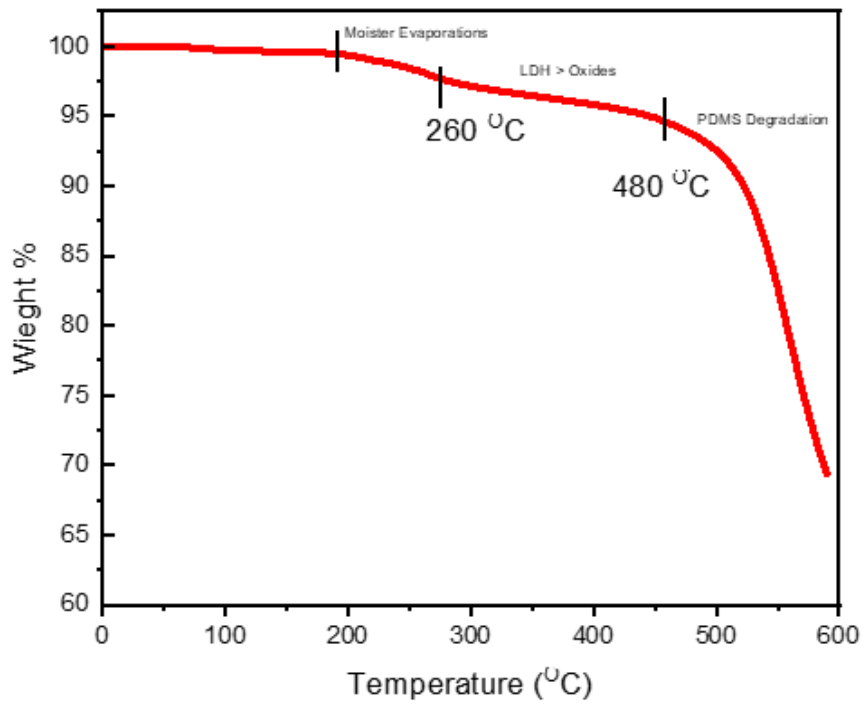


Figure 4.10: TGA graph of PDMS/ZnAl-LDH Composite sample.

Thermogravimetric analysis (TGA) is done to check the thermal stability of samples under extreme temperature conditions. As we see in **Figure 4.9** the pristine ZnAl-LDH is tends to degrade after 210 °C up to 490 °C while when fused or combined with PDMS its thermal stability increased and degradation point start 260 °C shown in **Figure 4.10**. During degradation LDH material is converted into oxides as shown in sample ZnAl-LDH and then it is converted into ZnO and Al<sub>2</sub>O<sub>3</sub> by products. PDMS coating gives strength to LDH helping in slower degradation in comparison with pristine LDH, because PDMS is a thermally stable material.

## 4.2 Electrical Characterizations

### 4.2.1 Fabrication of Triboelectric Nanogenerators

Principles of triboelectrification and electrostatic induction make the TENG operate. This is called triboelectrification where two materials are different such that they require different amounts of electrons to contact each other, thereby causing the first to acquire and the other to lose electrons. The materials surfaces become electrostatically charged as this process occurs.

#### **Design:**

The design of the Triboelectric Nanogenerator involves three different Triboelectric Nanogenerators (TENGs), each with distinct friction layer combinations:

- First TENG: PDMS (Polydimethylsiloxane)-based friction layers are formed as PDMS (Polydimethylsiloxane)/Al (aluminium sheet) friction layers. The aluminium back electrode is both the back electrode and the friction layer, to which the PDMS is coated.
- Second TENG: PDMS and ZnAl-LDH (LDH grown on aluminium) (PDMS/ZnAl-LDH) are both friction layers. Typically, ZnAl-LDH is grown on of aluminium, which in two roles: a friction layer and an electrode; the PDMS is the top friction layer.

- Third TENG: ZnAl-LDH coated with PDMS and an aluminium sheet (ZnAl-LDH/PDMS/Al) are used to form the friction layers. Aluminum is first patterned, on which a PDMS coating and ZnAl-LDH are deposited. In this configuration, the back electrode is aluminium sheet.

The friction layers for the three TENGs are mounted on acrylic substrates and separated by arc-shaped Polyamide (PI) sheets. Contact separation between these friction layers is also achieved in response to external mechanical forces because of this setup.

### **4.3 Electrical Characterization and Electronic Interface Circuit of the Triboelectric Nanogenerator**

#### *4.3.1 Electrical Characterization of Triboelectric Nanogenerator*

**Figure 4.11** shows the Triboelectric Nanogenerator prototype. The design has been found optimal for contact-separation of the friction layers due to an external mechanical stimulus. In order to electrically characterize the electrical output of the Triboelectric Nanogenerator, we first measured the output voltage  $V_{OC}$  at load resistance of  $1\text{ M}\Omega$  using oscilloscope due to hand tapping. The Triboelectric Nanogenerator produces a peak output voltage of  $\sim 31\text{ V}$ . I also characterized the short circuit current  $I_{SC}$  produced due to hand tapping as shown Fig. 30. This required a transimpedance preamplifier and oscilloscope. The Triboelectric Nanogenerator generates a peak  $I_{SC}$  of up to  $\sim 21\mu\text{A}$ . The Triboelectric Nanogenerator can be regarded as self-powered, it does not require external energy and indeed it generates electrical signals in response to a mechanical stimulus.

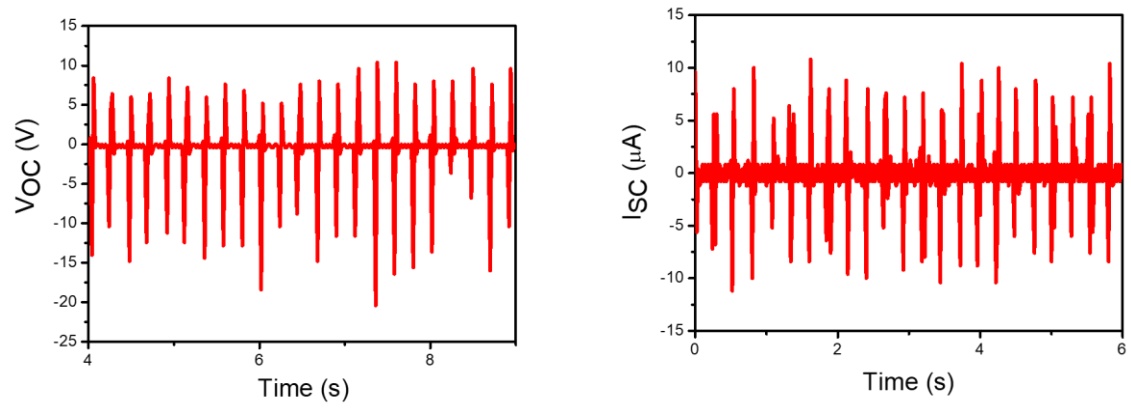


**Figure 4.11:** Graph of Output Voltage  $V_{OC}$  and Short circuit current  $I_{SC}$  of PDMS-AL TENG

In the **left graph**, the  $V_{oc}$  reaches peaks of around **31V**, with a series of sharp spikes over time. These peaks indicate the contact-separation cycles between the PDMS and aluminium layers, where triboelectric charging occurs due to repeated mechanical interaction. The consistent and repetitive pattern of the voltage peaks suggests efficient and stable triboelectric behavior, with effective charge transfer taking place as the layers make and break contact. The smooth and rapid voltage rise and fall show that the TENG is operating efficiently, converting mechanical energy into electrical energy.

The  $I_{sc}$  features sharp peaks that in right graph reach up to approximately **21 $\mu$ A**. The voltage peaks do indeed coincide with these current peaks, showing that the generation of current is driven mechanically by TENG mechanical interaction. When the layers come apart, the current spikes show that there is an effective transfer of triboelectric charges created on the surfaces. Based on the lower frequency of current peaks with respect to the voltage, it may be inferred that fewer cycles of contact and separation occurred over the same time period, perhaps due to the testing setup or Voltages and currents from sensors during tangling, and FE model calculations of equivalent stimuli.

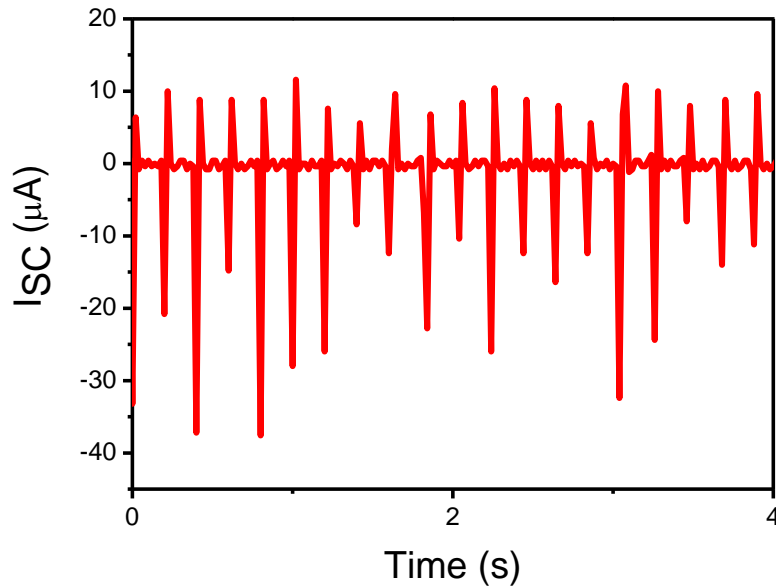


**Figure 4.12:** Short Circuit current  $I_{sc}$  of PDMS/ZnAl-LDH to Al TENG

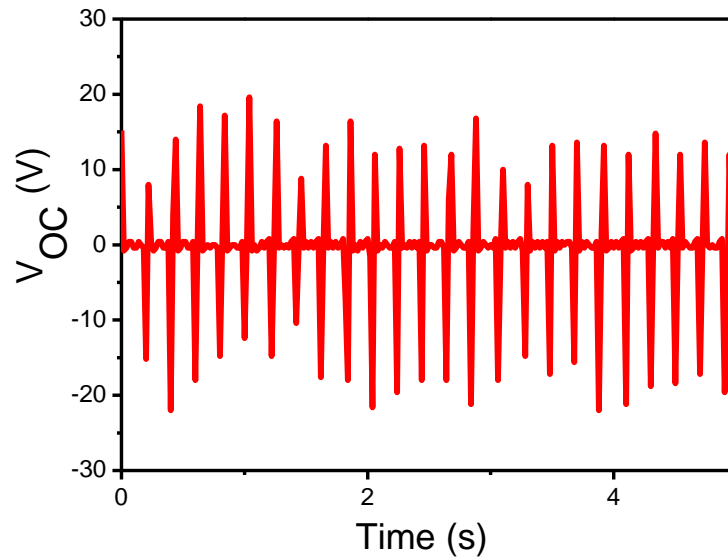


**Figure 4.13:** Output Voltage  $V_O$  at different load resistance for PDMS/ZnAl-LDH to Al TENG

The graphs provided illustrate the electrical performance of the PDMS-ZnAl-LDH Triboelectric Nanogenerator (TENG) in terms of short-circuit current ( $I_{sc}$ ) and open-circuit voltage ( $V_o$ ) under different load resistances.

In **Figure 4.12** the  $I_{sc}$  is shown over time. The current peaks at around **49 $\mu$ A**, indicating stable and consistent current generation due to the triboelectric effect between the PDMS and ZnAl-LDH layers. The repeated peaks are like the contact-separation cycles, where each cycle of mechanical energy applied to the TENG results in a sharp current generation. The consistent amplitude and frequency of the peaks suggest efficient charge transfer and collection, indicative of a robust triboelectric response from this TENG configuration.

In **Figure 4.13** presents the  $V_o$  of the TENG which I get is about 46 V Further in **Figure 4.14** I calculated  $V_o$  and  $I_o$  peak to peak at different load and make graph which follows the voltage-charge-displacement model of TENG and give us highest possible power we get from the device in which circumstances.

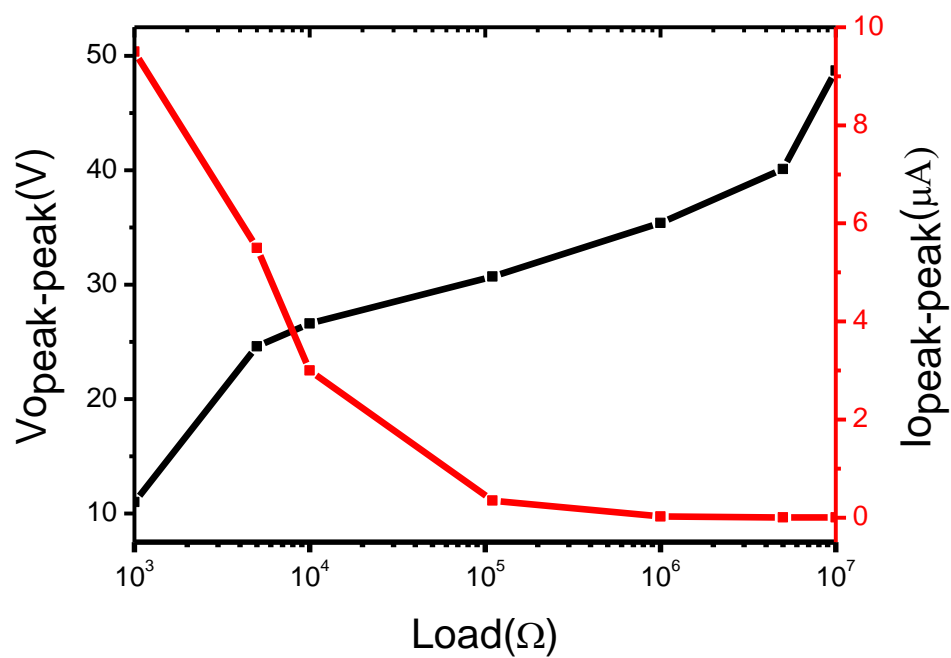


**Figure 4.14:**  $V_O$  and  $I_O$  at different Load of ZnAl-LDH/PDMS-Al TENG

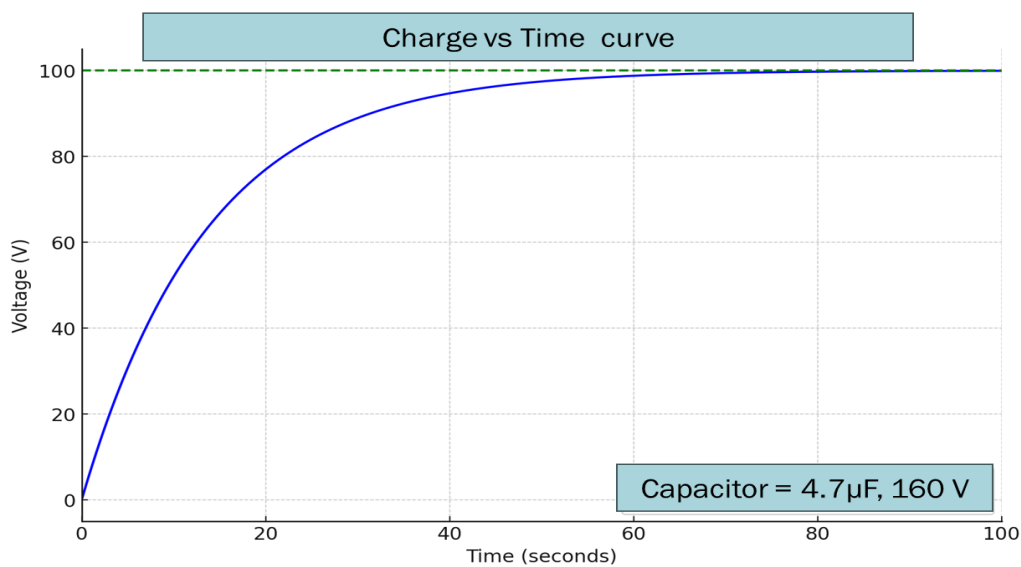


**Figure 4.15:** Charge Discharge graph for ZnAl-LDH/PDMS-Al TENG

In **Figure 4.15** graph provided here is the Charge vs Time curve for the ZnAl-LDH pressed into PDMS: Al triboelectric nanogenerator (TENG) and is charging into a 4.7  $\mu\text{F}$  capacitor with a rate of 160 V.

The voltage across this capacitor rises over time as the power generated by the ZnAl-LDH/PDMS TENG is captured by the ZnAl-LDH/PDMS TENG. It began at 0 V and increased curving until the maximum voltage is approximately 100 V. By the first few seconds, there is a rapid buildup of the voltage indicative of efficient TENG charging of the capacitor. The rate of increase slows down as time passes, and the voltage plateaus near 100 V, but it is slowing down, so they should soon stop increasing.

This charging pattern is exponential, which is typical of the charging of capacitors in a system. The ZnAl-LDH/PDMS to Al configuration is shown to have the ability to effectively harvest mechanical energy from the TENG to store the energy as electrical energy as the capacitor charges.

The plateau at around 100 V indicates that the TENG can charge the capacitor to a reasonable voltage allowing power to smaller energy devices, store energy for later retrieval, or a combination of both. This result illustrates the TENG's excellent energy storage performance, as the generated energy can be effectively captured and stored.

#### *4.3.2 Electronic Interface Circuit for Triboelectric Sensing of Biomechanical Motions*

TENG generate electrical signals in response to mechanical stimuli like hand tapping for example. However, these nanogenerators produce alternating-current (AC) pulses with high voltage and exceptionally low current ( $\sim\mu\text{As}$ ), which are incompatible with conventional electronics that require stable, low-voltage direct-current (DC) input. To bridge this gap, an electronic interface circuit is essential for connecting the triboelectric nanogenerator to conventional electronics.



#### 4.3.2.1 A. Electrical Equivalent of Triboelectric Nanogenerator

The triboelectric nanogenerator be capable of modeled as a voltage source in series with a variable capacitance[30], as depicted in bellow figure The voltage source is attributed to triboelectrification charges, while the variable capacitance arises from the air gap and the ZnAl-LDH dielectric between the top and bottom aluminum plates.

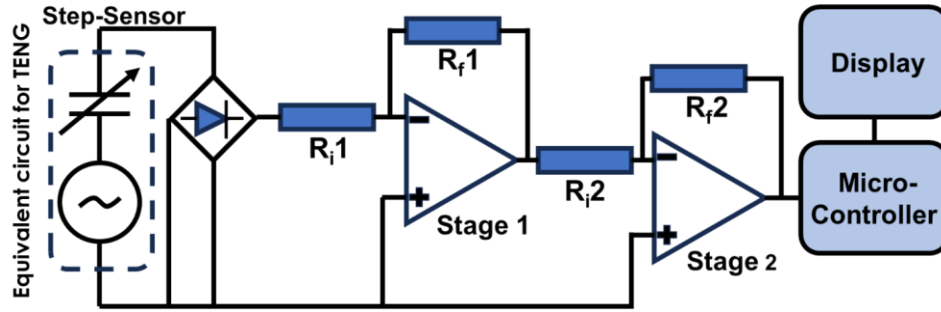


**Figure 4.16:** Schematic of Triboelectric equivalent circuit

#### 4.3.2.2 B. Two-Stage-Amplifier Based Electronic Interface Circuit

**Signal Rectification:** The AC signal produced by the triboelectric nanogenerator is first converted into DC using a full-wave bridge rectifier. This rectification is crucial for amplifying and processing the signal effectively [31, 32].

**Two-Stage Amplifier:** A two-stage amplifier, comprising two inverting amplifiers in series, is designed to interface the triboelectric nanogenerator with an Arduino Mega 2560 microcontroller[31, 32]. The first stage features a high input resistance to boost the voltage output, while the second stage provides additional gain to make the signal suitable for microcontroller detection. The gain of the two-stage amplifier  $A_V$  is calculated as follows:

$$A_V = \left(-\frac{R_{F1}}{R_{I1}}\right)\left(-\frac{R_{F2}}{R_{I2}}\right)$$

For the application  $R_{F1}$  and  $R_{I1}$  are 500 k $\Omega$  each, providing a gain of -1 for the first stage. The second stage, with  $R_{F2}$  and  $R_{I2}$  set to 10 k $\Omega$  and 1 k $\Omega$  respectively, offers a gain of -10. Consequently, the voltage pulses at the output range between 6 V and 10 V, which is suitable for microcontroller detection. The two-stage amplifier not only enhances the signal but also improves the signal-to-noise ratio (SNR) compared to single-stage amplifiers. The circuit is shown in **Figure 4.16**.

#### 4.4 Step Sensing Application

**Figure 4.17** illustrates the implementation of a PDMS/ZnAl-LDH contact-separation mode triboelectric nanogenerator (TENG) integrated into a step-sensing application. The TENG device, shown as part of a shoe in the lower section of the figure, is embedded within the sole, where it effectively converts mechanical energy from foot movement into electrical signals. This process relies on the contact and separation of PDMS and ZnAl-LDH layers, which generate a measurable triboelectric voltage due to the transfer of charge between the materials.

In the top-left section, the fabricated electronic circuit board is depicted. This circuit processes the output signal of the TENG using a series of amplification and filtering stages, as indicated in the schematic flowchart. The signal is then transmitted to a microcontroller for interpretation. The microcontroller calculates the number of steps based on the periodic signals generated during walking and displays the step count on the LCD screen, as demonstrated in the middle image. The successful integration of TENG-based energy harvesting and signal processing into a compact device underscores its potential for wearable electronics and self-powered sensors.

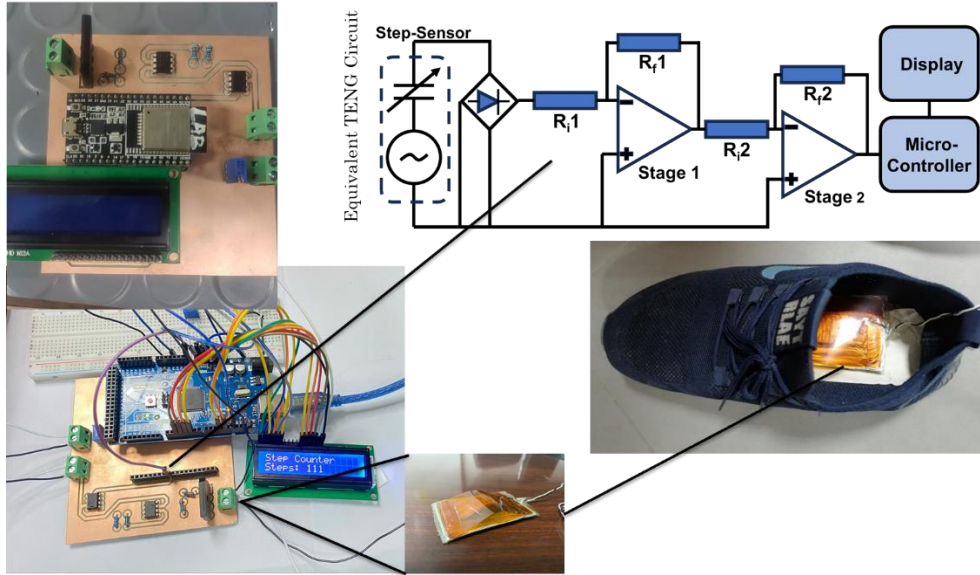


**Figure 4.17:** Digital camera image of integrated TENG in Shoe and tests for step sensing application

## CHAPTER 5: CONCLUSIONS AND FUTURE RECOMMENDATIONS

### 5.1 Conclusions

This research successfully developed and characterized triboelectric nanogenerators (TENGs) using both pristine PDMS and LDH/PDMS composites. XRD analysis confirmed the crystalline structure of ZnAl-LDH, with distinct peaks at the (003), (006), (009), and (110) planes, highlighting the well-ordered, layered nature of the material. SEM revealed that the ZnAl-LDH material exhibited a porous, nanostructured surface, which significantly increased the surface area after being used as a template for the PDMS coating.

Regarding the electrical functioning, the TENG with only the PDMS output voltage to about 31 V and a short circuit current of about 20  $\mu\text{A}$ . The triboelectric effect was markedly improved when ZnAl-LDH use as template and incorporated with PDMS, resulting in up to 40  $\mu\text{A}$  in short circuit current and peak voltage near 30 V. The better charge generation and transfer during the contact-separation process during the integration of the ZnAl-LDH template is assigned to the increasing surface roughness and surface area from the ZnAl-LDH template.

A 4.7  $\mu\text{F}$  capacitor energy storage tests were conducted with a ZnAl-LDH/PDMS based TENG, and it was demonstrated to be capable of charging the capacitor to 100 V within 100 s, suggesting its potential as an energy storage device. The combined effect of ZnAl-LDH template and PDMS coating on improving the triboelectric output and the total energy harvesting efficiency of the TENG is synergistic.

We ended with the utilization of ZnAl-LDH as a template to dramatically improve the surface area and triboelectric performance of the TENG. We obtained superior electrical performance and energy storage properties in the resulting ZnAl-LDH/PDMS TENG, and this TENG constitutes a promising candidate for sustainable energy harvesting systems. This composite material has the potential to be utilized for future applications as a small electronic power source or to collect environmental energy. The fabricated TENG device

was successfully demonstrated as a step-sensing application, showcasing its potential for real-life applications. Its ability to harvest biomechanical energy from footstep impacts highlights its practicality for smart sensing technologies. This development paves the way for integrating TENGs into wearable devices and energy-efficient monitoring systems.

## **5.2 Future Recommendations**

Future work should focus on further optimizing the design and fabrication process of LDH/PDMS-based TENGs to enhance their scalability and integration into practical energy harvesting systems. Exploring other LDH materials with varying compositions, such as MgAl-LDH or NiAl-LDH, could provide additional benefits in terms of surface properties and charge generation. Moreover, the development of flexible and wearable TENGs for real-world applications, such as powering small electronics or environmental sensors, should be investigated. Lastly, improving the energy storage capacity and developing hybrid systems that combine TENGs with other energy harvesting technologies could maximize overall energy efficiency and broaden the range of potential applications.

## REFERENCES

1. Walden, R., et al., *Opportunities and challenges in triboelectric nanogenerator (TENG) based sustainable energy generation technologies: a mini review*. Chemical Engineering Journal Advances, 2022. **9**: p. 100237.
2. Cheng, T., J. Shao, and Z.L. Wang, *Triboelectric nanogenerators*. Nature Reviews Methods Primers, 2023. **3**(1): p. 39.
3. Niu, X., et al., *High-performance PZT-based stretchable piezoelectric nanogenerator*. ACS Sustainable Chemistry & Engineering, 2018. **7**(1): p. 979-985.
4. Sezer, N. and M. Koç, *A comprehensive review on the state-of-the-art of piezoelectric energy harvesting*. Nano energy, 2021. **80**: p. 105567.
5. Carneiro, P., et al., *Electromagnetic energy harvesting using magnetic levitation architectures: A review*. Applied Energy, 2020. **260**: p. 114191.
6. Beeby, S.P. and T. O'Donnell, *Electromagnetic energy harvesting*. Energy Harvesting Technologies, 2009: p. 129-161.
7. Niu, S. and Z.L. Wang, *Theoretical systems of triboelectric nanogenerators*. Nano Energy, 2015. **14**: p. 161-192.
8. Cheng, T., Q. Gao, and Z.L. Wang, *The current development and future outlook of triboelectric nanogenerators: a survey of literature*. Advanced Materials Technologies, 2019. **4**(3): p. 1800588.
9. Kim, W.-G., et al., *Triboelectric nanogenerator: Structure, mechanism, and applications*. ACS nano, 2021. **15**(1): p. 258-287.
10. Zou, H., et al., *Quantifying the triboelectric series*. Nature communications, 2019. **10**(1): p. 1427.
11. Hasan, S., et al., *Comparative study on the contact-separation mode triboelectric nanogenerator*. Journal of electrostatics, 2022. **116**: p. 103685.
12. Wang, Z.L., et al., *Triboelectric nanogenerator: Lateral sliding mode*. Triboelectric nanogenerators, 2016: p. 49-90.
13. Wang, Z.L., et al., *Triboelectric nanogenerator: single-electrode mode*. 2016: Springer.

14. Wang, Z.L., et al., *Triboelectric nanogenerator: Freestanding triboelectric-layer mode*. *Triboelectric Nanogenerators*, 2016: p. 109-153.
15. Liu, J., et al., *Synthesis and thermal properties of ZnAl layered double hydroxide by urea hydrolysis*. *Powder technology*, 2014. **253**: p. 41-45.
16. Iyi, N., Y. Ebina, and T. Sasaki, *Water-swellable MgAl-LDH (layered double hydroxide) hybrids: synthesis, characterization, and film preparation*. *Langmuir*, 2008. **24**(10): p. 5591-5598.
17. Shivashankar, H., et al., *Investigation on dielectric properties of PDMS based nanocomposites*. *Physica B: Condensed Matter*, 2021. **602**: p. 412357.
18. Trinh, V. and C. Chung, *Harvesting mechanical energy, storage, and lighting using a novel PDMS based triboelectric generator with inclined wall arrays and micro-topping structure*. *Applied Energy*, 2018. **213**: p. 353-365.
19. Barras, R., et al., *Porous PDMS conformable coating for high power output carbon fibers/ZnO nanorod-based triboelectric energy harvesters*. *Nano Energy*, 2021. **90**: p. 106582.
20. Raseel, M.S.U. and J.-Y. Park, *A sandpaper assisted micro-structured polydimethylsiloxane fabrication for human skin based triboelectric energy harvesting application*. *Applied energy*, 2017. **206**: p. 150-158.
21. Ren, X., et al., *Flexible lead-free BiFeO<sub>3</sub>/PDMS-based nanogenerator as piezoelectric energy harvester*. *ACS applied materials & interfaces*, 2016. **8**(39): p. 26190-26197.
22. Yoon, C., et al., *Synergistic contribution of flexoelectricity and piezoelectricity towards a stretchable robust nanogenerator for wearable electronics*. *Nano Energy*, 2022. **91**: p. 106691.
23. Prestopino, G., et al., *Layered-Double-Hydroxide (LDH) pyroelectric nanogenerators*. *Nano Energy*, 2023. **118**: p. 109017.
24. Sohn, S.H., et al., *Synergistic Coupling of Tribovoltaic and Moisture-Enabled Electricity Generation in Layered-Double Hydroxides (Adv. Energy Mater. 10/2024)*. *Advanced Energy Materials*, 2024. **14**(10): p. 2470044.
25. Mohsom, P., et al., *Advanced Composite Triboelectric Nanogenerator from Bacterial Cellulose and MgAl-LDH Nanosheets: Synthesis, Performance, and Mechanistic insight*. 2024.
26. Mondal, A., et al., *Double-Layer Electronegative Structure-Based Triboelectric Nanogenerator for Enhanced Performance Using Combined Effect of Enhanced*

- Charge Generation and Improved Charge Trapping*. ACS Applied Materials & Interfaces, 2024. **16**(38): p. 50659-50670.
27. Wu, Y., et al., *Piezoelectric materials for flexible and wearable electronics: A review*. Materials & Design, 2021. **211**: p. 110164.
  28. Tajuddin, N., et al., *Hydrothermal Reconstructing Routes of Alkali-Free ZnAl Layered Double Hydroxide: A Characterisation Study*. Solid State Phenomena, 2019. **290**: p. 168-176.
  29. Berthomieu, C. and R. Hienerwadel, *Fourier transform infrared (FTIR) spectroscopy*. Photosynthesis research, 2009. **101**: p. 157-170.
  30. Zhao, P., *Design of high-performance Triboelectric Nanogenerators (TENGs) for energy harvesting applications*. 2020, University of Bolton.
  31. Lu, S., et al., *Regulating the high-voltage and high-impedance characteristics of triboelectric nanogenerator toward practical self-powered sensors*. Nano Energy, 2021. **87**: p. 106137.
  32. Mallineni, S.S.K., et al., *A low-cost approach for measuring electrical load currents in triboelectric nanogenerators*. Nanotechnology Reviews, 2018. **7**(2): p. 149-156.
  33. Liu, R. and M. Li, *A textile-based triboelectric nanogenerator for long jump monitoring*. Materials Technology, 2022. **37**(12): p. 2360-2367.
  34. Xia, K., et al., *A high-output triboelectric nanogenerator based on nickel–copper bimetallic hydroxide nanowrinkles for self-powered wearable electronics*. Journal of Materials Chemistry A, 2020. **8**(48): p. 25995-26003.
  35. He, S., et al., *A self-powered  $\beta$ -Ni (OH) <sub>2</sub>/MXene based ethanol sensor driven by an enhanced triboelectric nanogenerator based on  $\beta$ -Ni (OH) <sub>2</sub>@ PVDF at room temperature*. Nano Energy, 2023. **107**: p. 108132.
  36. Xu, M., et al., *A highly-sensitive wave sensor based on liquid-solid interfacing triboelectric nanogenerator for smart marine equipment*. Nano Energy, 2019. **57**: p. 574-580.
  37. Fan, Y.J., et al., *Stretchable porous carbon nanotube-elastomer hybrid nanocomposite for harvesting mechanical energy*. Advanced Materials, 2017. **29**(2): p. 1603115.
  38. Xie, J., Z. Khalid, and J.M. Oh, *Recent advances in the synthesis of layered double hydroxides nanosheets*. Bulletin of the Korean Chemical Society, 2023. **44**(2): p. 100-111.



39. Chengqian, F., et al., *One-step coprecipitation synthesis of Cl–intercalated Fe<sub>3</sub>O<sub>4</sub>@ SiO<sub>2</sub>@ MgAl LDH nanocomposites with excellent adsorption performance toward three dyes*. Separation and Purification Technology, 2022. **295**: p. 121227.
40. Tajat, N., et al., *Utilization of Zn–Al–Cl layered double hydroxide as an adsorbent for the removal of anionic dye Remazol Red 23 in aqueous solutions: kinetic, equilibrium, and thermodynamic studies*. Nanotechnology for Environmental Engineering, 2022. **7(2)**: p. 343-357.
41. Huang, C., et al., *One-step hydrothermal synthesized 3D P–MoO<sub>3</sub>/FeCo LDH heterostructure electrocatalysts on Ni foam for high-efficiency oxygen evolution electrocatalysis*. International Journal of Hydrogen Energy, 2021. **46(24)**: p. 12992-13000.
42. Prabagar, J.S., et al., *Photocatalytic transfer of aqueous nitrogen into ammonia using nickel-titanium-layered double hydroxide*. Environmental Science and Pollution Research, 2023. **30(39)**: p. 90341-90351.
43. Smalenskaite, A., et al., *Sol–gel synthesis and characterization of coatings of Mg-Al layered double hydroxides*. Materials, 2019. **12(22)**: p. 3738.
44. Valeikiene, L., et al., *Investigation of Structural and Luminescent Properties of Sol-Gel-Derived Cr-Substituted Mg<sub>3</sub>Al<sub>1-x</sub>Cr<sub>x</sub> Layered Double Hydroxides*. Molecules, 2021. **26(7)**: p. 1848.
45. Chen, Z., et al., *Synthesis of two-dimensional layered double hydroxides: a systematic overview*. CrystEngComm, 2022. **24(26)**: p. 4639-4655.
46. Mao, N., et al., *Exfoliation of layered double hydroxide solids into functional nanosheets*. Applied Clay Science, 2017. **144**: p. 60-78.
47. Morales, D.M., et al., *Enhancing Electrocatalytic Activity through Liquid-Phase Exfoliation of NiFe Layered Double Hydroxide Intercalated with Metal Phthalocyanines in the Presence of Graphene*. ChemPhysChem, 2019. **20(22)**: p. 3030-3036.
48. Liu, J., et al., *Synthesis and thermal properties of ZnAl layered double hydroxide by urea hydrolysis*. Powder technology, 2014. **253**: p. 41-45.
49. Ahmed, A.A.A., Z.A. Talib, and M.Z. bin Hussein, *Thermal, optical and dielectric properties of Zn–Al layered double hydroxide*. Applied Clay Science, 2012. **56**: p. 68-76.
50. Johnston, A.-L., et al., *Understanding Layered Double Hydroxide properties as sorbent materials for removing organic pollutants from environmental waters*. Journal of Environmental Chemical Engineering, 2021. **9(4)**: p. 105197.

